Review of Failure Criteria for Thin Wall Structures in a High Heat Flux Environment

Bruce B. Glasgow

March 1985

UWFDM-633

FUSION TECHNOLOGY INSTITUTE

UNIVERSITY OF WISCONSIN

MADISON WISCONSIN

Review of Failure Criteria for Thin Wall Structures in a High Heat Flux Environment

Bruce B. Glasgow

Fusion Technology Institute
University of Wisconsin
1500 Engineering Drive
Madison, WI 53706

http://fti.neep.wisc.edu

March 1985

UWFDM-633

REVIEW OF FAILURE CRITERIA FOR THIN WALL STRUCTURES IN A HIGH HEAT FLUX ENVIRONMENT

Bruce B. Glasgow

Fusion Technology Institute
1500 Johnson Drive
University of Wisconsin-Madison
Madison, Wisconsin 53706

March 1985

UWFDM-633

REVIEW OF FAILURE CRITERIA FOR THIN WALL STRUCTURES IN A HIGH HEAT FLUX ENVIRONMENT

Introduction

The first wall components of fusion reactors will be subjected to a severe environment including 14 MeV neutrons, energetic particles, pulsed high heat fluxes, and corrosive coolants. It is believed that the life-limiting processes for the first wall structures will be crack propagation and subsequent failure by either leak-through or brittle fracture. Also, because of the thin structures to be used in fusion first walls, plastic collapse may be of importance.

This paper is a review of the various aspects of crack propagation and failure criteria for thin wall structures. An extensive review of past work is presented and recommendations are made as to crack propagation models and failure criteria.

This review was prepared for the preliminary examination of Bruce B. Glasgow.

TABLE OF CONTENTS

EFFECTS OF RADIATION AND HIGH HEAT FLUX ON THE PERFORMANCE OF FIRST WALL COMPONENTS IN FUSION REACTORS

Bruce B. Glasgow

Department of Nuclear Engineering, 1500 Johnson Drive
University of Wisconsin-Madison, Madison, Wisconsin 53706

Preliminary Examination for Doctoral Research

August 1983

ABSTRACT

The first wall components of fusion reactors will be subjected to a severe environment including 14 MeV neutrons, energetic particles, pulsed heat fluxes, and corrosive coolants. Because of the high heat fluxes, the first wall components will probably have to be thin-walled structures. It is believed that the growth of flaws or cracks to a critical size will be the dominant failure mechanism for first wall components. It is proposed to develop a structural analysis code for first wall components to evaluate structural and materials performance. Two existing codes, WISECRACK and TSTRESS, developed at the University of Wisconsin-Madison, will be modified to accomplish this task.

1. STATEMENT OF PROBLEM

First wall components such as limiters, beam dumps, divertor plates, and the first wall itself will probably have to be thin-walled structures because of the high energy flux to which they are exposed. The first wall components may also be subjected to a severe environment including 14 MeV neutrons, energetic particles, pulsed heat fluxes, and corrosive coolants.

1.1 Introduction

Some general features of first wall components which can influence their lifetime are as follows.

1. The high heat flux makes thermal stresses a major load source; and thus, a thin-walled structure is desirable.
2. Differential swelling, irradiation creep, and thermal stresses must be accounted for in determining the fatigue loadings.
3. Erosion, corrosion, radiation induced embrittlement, and fatigue/creep crack growth may determine the eventual failure mode.

A crack, no matter how small, could grow to sufficiently large size to compromise the integrity of the first wall. It is therefore proposed that the research for this author be concentrated in the area of calculating crack growth rates for a fusion reactor first wall. The research will include:

1. Development of a structural analysis code for any first wall component which can be represented by a shell.
2. Determination of relevant material properties as a function of temperature and irradiation.
3. Determination of thermal stresses in the first wall including creep relaxation effects.

4. Determination of crack growth rates from fatigue, creep, corrosion, etc.
5. Determination of the effective lifetime of a first wall due to crack growth and subsequent failure by plastic collapse, brittle fracture, or leak-through.

A more detailed discussion of selected topics follows in later chapters.

1.2 Background

By coupling an inelastic stress analysis to fatigue crack growth in the UWMAK-I blanket module first wall, the first integrated lifetime analysis was performed.[1-3] The results identified flaw growth as the life limiting failure mechanism. A finite element code, ANSYS, was used to calculate the 2-D stress history due to irradiation creep, swelling, and plasticity. This was coupled to a 1-D crack growth calculation of a surface flaw. However, the most serious omission from this study was the effect of embrittlement in the fracture mechanics analysis. Wall erosion was also omitted.

Another important study is the lifetime analysis done by Wolfer and Watson[4] for a graphite first wall structure. Wolfer and Watson integrated the reduction in fracture strength due to porosity changes with a 1-D inelastic stress analysis to compute brittle fracture lifetime. No crack growth or erosion was considered.

Another significant lifetime study is the analysis of the Westinghouse cylindrical blanket module done by Prevenslick.[5] Particularly notable is the detailed structural analysis done with a 1-D ANSYS inelastic model. Prevenslick was the first to include creep crack growth and a drop in fracture toughness due to irradiation.

Surface erosion effects were considered separately[6] in the fatigue analysis of the INTOR first wall. It was found that by including the reduction

in cyclic thermal stresses due to wall thinning, the fatigue life could be extended from 4×10^5 cycles to greater than 1×10^7 cycles. No crack growth calculations were done for the design, however.

Another important study is the lifetime analysis of the STARFIRE first wall.[7] That study is significant because it integrated a 2-D inelastic stress analysis with a crack growth analysis. However, the study neglected wall erosion and neutron embrittlement.

Finally, it should be noted that none of the above studies included any threshold effects on fatigue crack propagation, effects of embrittlement on fatigue crack growth, or effects of wall erosion on crack propagation.

The most extensive work done in the area of fusion reactor first wall lifetime has been done by Watson.[8] The basic computer code to be used for this research is, in fact, the WISECRACK code written by Watson. In the current version of the code the first wall is modeled as a flat plate containing a small semi-elliptical surface crack. The plate is subjected to membrane loads, cyclic heat fluxes, irradiation creep and swelling, embrittlement, and surface erosion and corrosion. Failure occurs when either the crack propagates through the wall (leak-through) or when brittle fracture occurs.

Improvements in the lifetime analysis will include: (1) modeling the first wall as a shell subjected to membrane and bending loads, (2) prediction of failure when leak-through occurs or when the "CEGB R6" requirement is violated (to be discussed in a later chapter), and (3) the current version of WISECRACK models only 316 stainless steel; the code will be revised to model ferritic steel as well.

One of the major conclusions Watson made using the current version of the WISECRACK code is that the lifetime is approximately inversely proportional to

the fourth power of the cyclic thermal stresses. If this conclusion can be applied to ferritic steels, it is expected that the lifetime will increase dramatically by the use of ferritic steels. Young's modulus E and the coefficient of thermal expansion α are both smaller for ferritic steels; therefore, thermal stresses will be less. Another major improvement to the WISECRACK code will be the allowance of bending (as opposed to the current model of a plate constrained from bending). Wolfer reports[9] that for a plate, there is a factor of 20 reduction in the thermal stresses when the plate is allowed to bend. The improvement should also result in a greatly improved lifetime.

Another existing code which will be used is the TSTRESS code written by Peterson, Watson, Wolfer, and Moses.[10] TSTRESS performs a 1-D inelastic stress analysis of a thin, clamped plate subjected to a heat flux. Thermal and irradiation creep relaxation and irradiation swelling are included. Modifications to TSTRESS will include: (1) modeling the wall as a shell, (2) including ferritic steel as well as 316 stainless steel.

2. THEORY AND PREDICTION OF FATIGUE CRACK PROPAGATION

The problem of fatigue crack propagation and the development of various empirical equations to predict fatigue crack propagation rates are discussed. Also, the theory of fatigue crack propagation is reviewed. Finally, a recommendation is made regarding the prediction of fatigue crack propagation rates as they apply to fusion reactor first walls.

2.1 Introduction

When stress is cyclic (that is, involving stress or strain reversals), such as occurs during testing and transient operations, all stresses become significant and contribute in establishing the "fatigue life" of a component, even if the material involved is a ductile one. Fatigue life has been evaluated by comparing the amplitude of the alternating stress intensity with that from design fatigue curves (SN curves) experimentally established for the material. A typical SN curve for a carbon steel is shown in Fig. 1 and can be expressed by the equation[11]

$$S_a = \frac{E}{4N^{1/2}} \ln \left\{\frac{100}{100 - RA}\right\} + 0.35\ TS \qquad (1)$$

where: S_a = value of alternating stress intensity amplitude

E = Young's modulus

N = number of cycles

RA = reduction in area

TS = tensile strength.

Typical constant stress amplitude fatigue cycles are presented in Fig. 2.

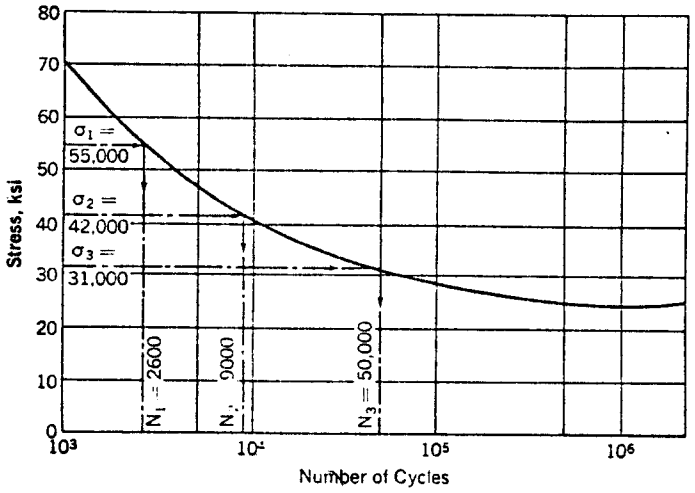

Fig. 1. Fatigue evaluation.[11]

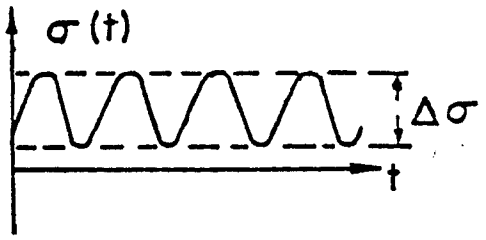

Fig. 2. Typical stress cycle for fatigue testing.[8]

For many years fatigue life tests were conducted by using a stress cycle similar to that shown in Fig. 2. The test was conducted until failure occurred. The data were plotted as stress (S) versus number of cycles to failure (N) as shown in Fig. 1. This SN curve was, and is, used extensively for evaluating fatigue behavior of materials and structures. It wasn't until the 1950's and 1960's that it was recognized that the fatigue failures were initiating from either a design discontinuity or a metallurgical defect of some type. It is now thought that the fatigue process can be divided into three

parts: (1) initiation of a crack at a discontinuity or defect, (2) propagation of the crack, and (3) failure. This section concentrates on describing the second part of the fatigue process -- propagation.

While some design philosophies specify that the useful life of a structure is until the onset of crack initiation, it is not clear to this author that the crack initiation criterion is appropriate. For example, additional life for the component can be realized by including the crack propagation lifetime. On the other hand, a preexistent crack may propagate to failure before experiments would show that a smooth specimen would initiate a crack.

An additional concern for fatigue crack propagation (FCP) is the possibility of a crack propagating to a critical size to cause a failure other than fatigue failure. Flaws which can exist at manufacture or which could develop in time may not be large enough to cause brittle failure or plastic collapse of the structure. However, such subcritical cracks can grow during service due to fatigue. This FCP can result in large cracks of sufficient size to cause failure by brittle fracture, or by plastic collapse, or by a leak-through when the crack propagates across the section thickness.

The remainder of this section discusses the various empirical equations used to predict FCP rates. Finally, there is a short discussion on the rather underdeveloped area concerning the theory of FCP.

2.2 The Paris Equation

The rate of FCP, da/dN, can be defined as the amount of crack extension caused by cyclic stresses within a single load cycle. FCP has been correlated well with the stress intensity factor range, ΔK, where $\Delta K = K_{max} - K_{min}$ (recall that $K = \sigma(\pi a)^{1/2}$ for a through-thickness crack). For most metals, a plot of experimental da/dN data versus ΔK can be divided into three regimes as

shown in Fig. 3. The stage I regime, or threshold regime, is characterized by a rapid decrease in da/dN as ΔK becomes smaller, until ΔK reaches some ΔK_o, the threshold value where da/dN becomes vanishingly small. ΔK_o is considered a material property. In stage II, the stable growth regime, the slope of the curve is relatively constant and the data can be fit to the basic Paris Law proposed in 1963 by Paris and Erdogan[12]

$$\frac{da}{dN} = C(\Delta K)^n \tag{2}$$

where C and n are constants. Finally, stage III, the unstable regime, is marked by rapidly increasing crack growth as ΔK approaches K_{Ic}, the plane strain fracture toughness (also a material property).

2.3 Effect of R-Ratio

While the Paris equation is the foundation of predictions of FCP rates, additional parameters must be included in order to better fit the available data. One of the parameters to be considered is the effect of the mean stress, $(\sigma_{max} + \sigma_{min})/2$. It has been found that increasing the mean cyclic stress also increases the FCP rate. In order to model the effect of the mean cyclic stress, first some quantities must be defined as:

$$K_{mean} = \frac{K_{max} + K_{min}}{2} \tag{3}$$

$$R = \frac{K_{min}}{K_{max}} \tag{4}$$

or upon rearranging the above two equations

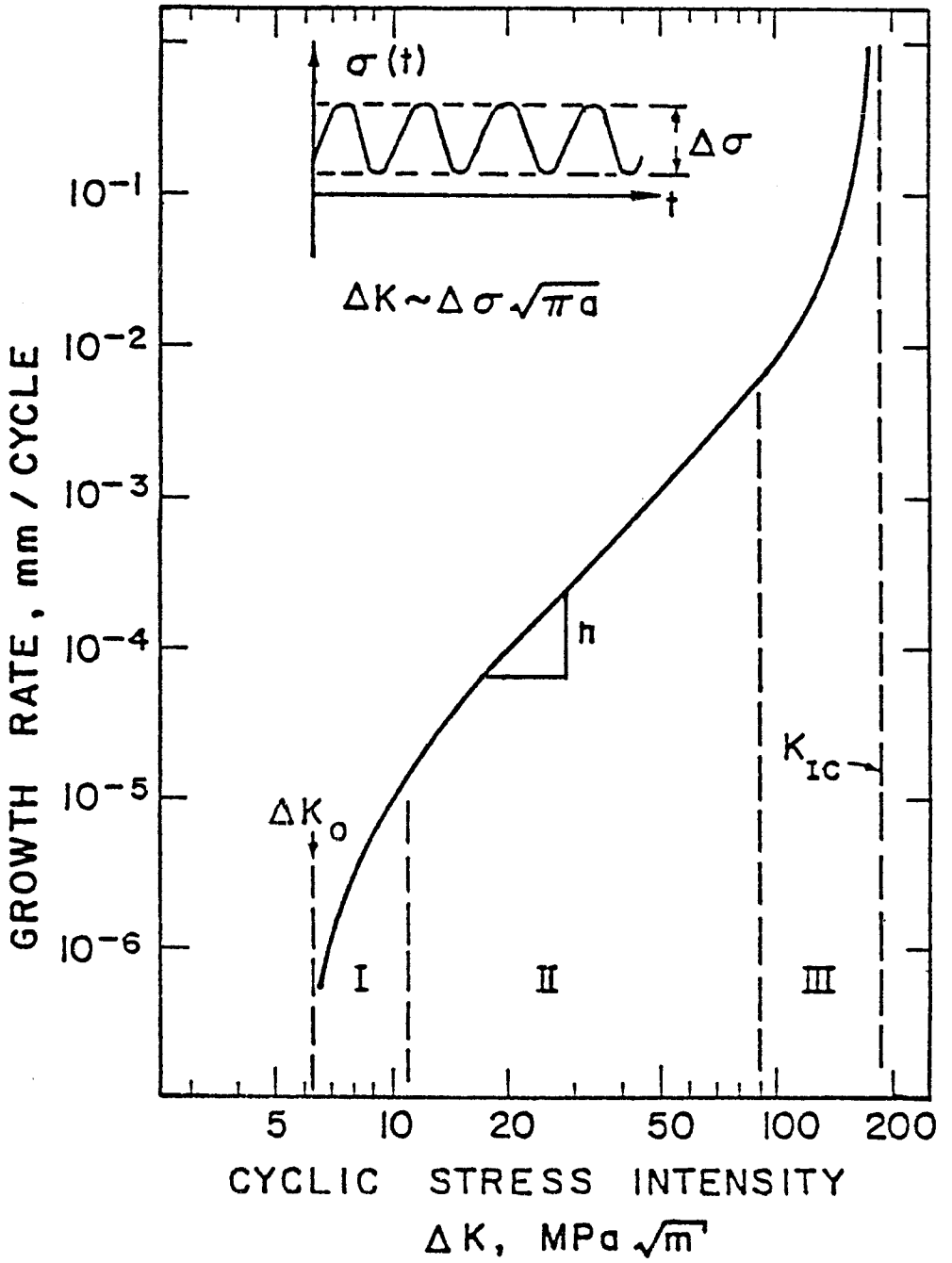

Fig. 3. Schematic of three stages of fatigue crack growth behavior. Stage I is the threshold regime. Stage II is the linear, stable growth regime, and Stage III is the unstable, fast growth/fracture regime.[8]

$$K_{mean} = \frac{1}{2} \Delta K \frac{1 + R}{1 - R} . \quad (5)$$

One of the first ways proposed to incorporate the effect of the mean cyclic stress (or R-ratio) was proposed by Walker[13] in 1970. Walker proposed the equation

$$\frac{da}{dN} = C[K_{max}(1 - R)^m]^n \quad (6)$$

where C, m, n are all constants to be fit to the data. R is the R-ratio related to the mean cyclic stress as defined above. Another correlation to account for the R-ratio effect was proposed by Sullivan and Crooker.[14] Their proposed equation has the form

$$\frac{da}{dN} = A\Delta K^n \frac{1 - bR}{1 - R} \quad (7)$$

where A, b, and n are fit to the data. A plot of the Sullivan et al. fit is shown in Fig. 4. Other corrections for the R-ratio effect have been proposed; one of these will be presented in a later section.

2.4 Effect at Low ΔK

An additional parameter to be considered in order to match the experimental data to an equation is the apparent threshold ΔK, ΔK_o. As can be seen in Fig. 3, da/dN approaches zero as ΔK approaches ΔK_o. Two simple ways of incorporating this behavior were proposed by Klesnil and Lukas in 1971[15] and by Speidel in 1974.[16] These are

$$\frac{da}{dN} = C(\Delta K^n - \Delta K_o^n) \quad (8)$$

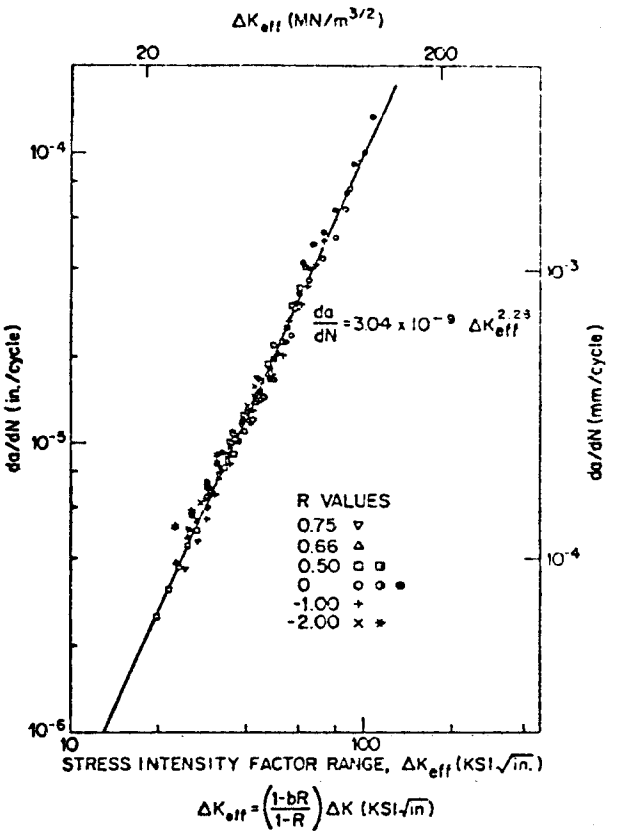

Fig. 4. Control data normalized using the effective stress function $\Delta K_{eff} = ((1 - bR)/1R)\ \Delta K$ ksi $\sqrt{in.}$ where b = 0.85 R > 0 and 1.40 R < 0.[14]

and

$$\frac{da}{dN} = (C\Delta K - \Delta K_o)^n \qquad (9)$$

where again C and n are constants. ΔK_o is assumed to be a material property. An example of a fit to the first equation where n = 2, done by Donahue, Clark, Atanmo, Kumble, and McEvily,[17] is shown in Fig. 5.

2.5 Effect of R-Ratio on ΔK_o

It has also been found that the threshold ΔK, ΔK_o, is not a constant of only the material. Instead, ΔK_o appears to be a linear function of the R-

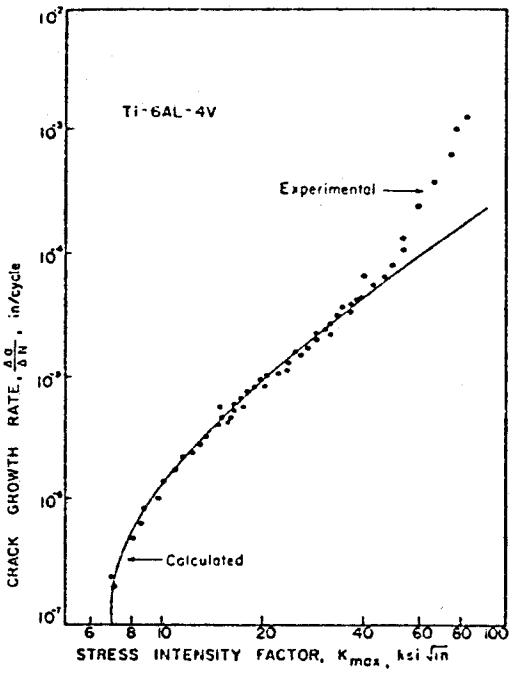

Fig. 5. Comparison of calculated best fit curve and experimental crack growth data for Ti-6Al-4V at 80°F.[17]

ratio as well. Figure 6 shows the results Ritchie[18] obtains for da/dN versus ΔK at different R-ratios. In 1974 Barsom[19] suggested that, based on the available data, ΔK_o could be correlated by

$$\Delta K_o = \Delta K_{oo}(1 - bR) \tag{10}$$

where ΔK_{oo} is the threshold ΔK at R = 0 and b is a fitted constant. Vosikovsky[20] also showed that such a straight line correlation between ΔK_o and the R-ratio exists, as shown in Fig. 7. For steels there is a general trend of decreasing ΔK_o with increasing R-ratio; for negative R-ratios the sensitivity appears to be less. Watson[8] reports that a fit to stainless

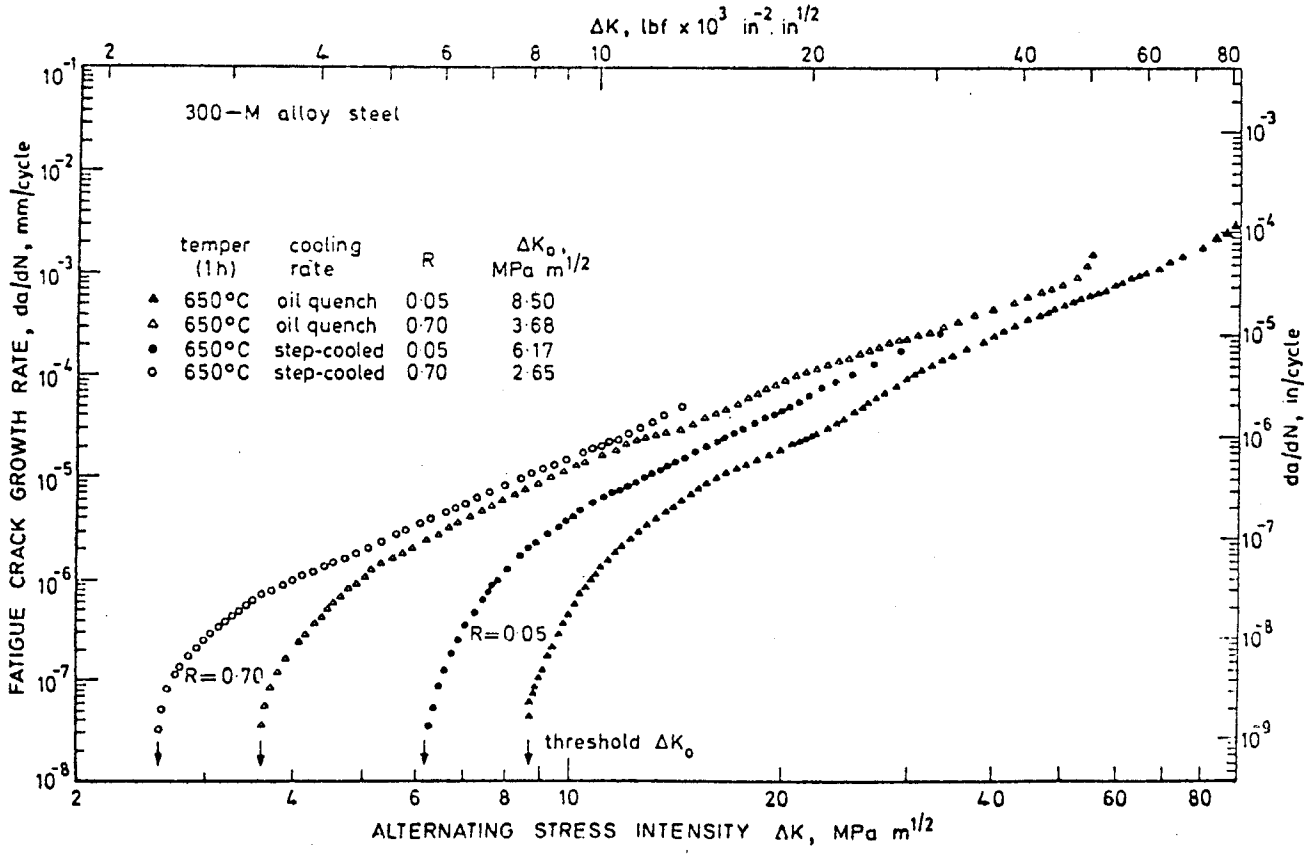

Fig. 6. Fatigue crack propagation results for 300-M, oil-quenched (T650) and step-cooled (T650SC) after tempering at 650°C.[18]

steel data results in

$$\Delta K_o = 5.4(1 - 0.9\ R) \qquad (11)$$

for $R < 0$, and

$$\Delta K_o = 5.4\ (1 - 0.2\ R) \qquad (12)$$

for $R > 0$.

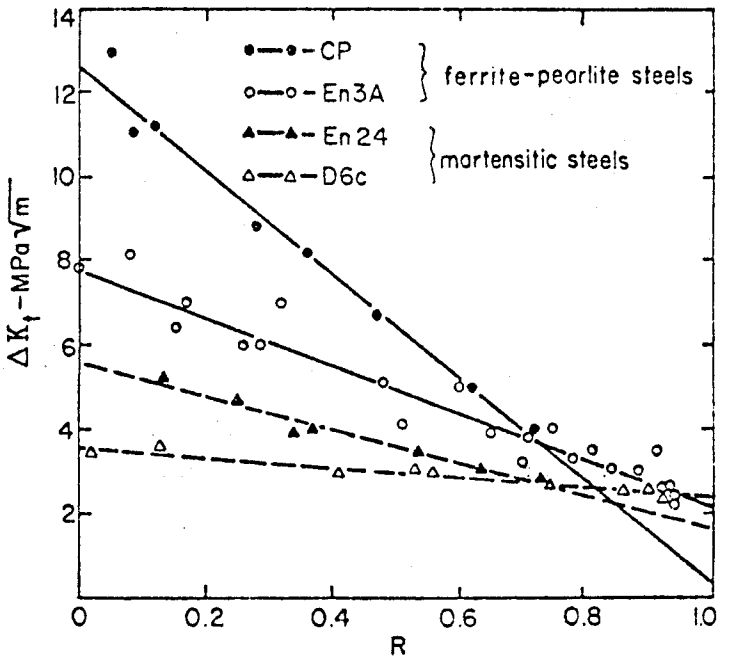

Fig. 7. The dependence of thresholds on stress ratio for four steels with the most extensive threshold measurements.[20]

2.6 Small Crack Correction

Most of the experimental data prior to 1975 was obtained with crack lengths greater than 1 mm. Pearson[21] first observed that smaller cracks tend to grow at a faster rate than predicted by the current empirical relationships. This observation has led to a short crack correction.

Two possible reasons for the short crack effect have been proposed. First, Talug and Reifsnider[22] concluded that crack tip stresses for small cracks are increased over crack tip stresses for larger cracks. This would result in a larger ΔK and hence a larger da/dN. Second, continuum mechanics may no longer apply in the region around such a small crack; therefore, predictions of the stress field ahead of the crack may be incorrect.

In any case, El Haddad, Smith and Topper[23,24] developed a simple scheme. El Haddad et al. recommended replacing the actual crack length, a, with an effective length, a_{eff}, according to $a_{eff} = a + l_o$. As a becomes larger, l_o becomes negligible. To determine l_o first consider

$$\Delta K = \Delta\sigma[\pi(a + l_o)]^{1/2} \tag{13}$$

now at the threshold ΔK

$$\Delta K_o = \Delta\sigma_o[\pi(a + l_o)]^{1/2} \tag{14}$$

where $\Delta\sigma_o$ is the cyclic stress where cracks will not propagate. Then solving for $\Delta\sigma_o$

$$\Delta\sigma_o = \frac{\Delta K_o}{\pi(a + l_o)^{1/2}} . \tag{15}$$

Taking the limit as "a" goes to zero, one obtains

$$\Delta\sigma_e = \frac{\Delta K_o}{(\pi l_o)^{1/2}} \tag{16}$$

where $\Delta\sigma_e$ is the smooth specimen fatigue cyclic stress limit which is known for materials. Therefore

$$l_o = \frac{1}{\pi}\left(\frac{\Delta K_o}{\Delta\sigma_e}\right)^2 . \tag{17}$$

For 316 stainless steel $l_o \sim 0.064$ mm. El Haddad et al. present their results

in Figs. 8 and 9 for the cases without and with short crack corrections, respectively.

2.7 Effect at High ΔK

At high ΔK, where ΔK is approaching K_{Ic}, the ΔK dependence of crack growth increases markedly. Forman, Kearney and Engle[25] proposed in 1967 what has come to be known as the Forman equation:

$$\frac{da}{dN} = \frac{C\Delta K^n}{(1 - R)K_{Ic} - \Delta K} \cdot \tag{18}$$

Figure 10 shows the good agreement of the Forman equation with the data. However, in order to even better match the available data, Nordberg[26] in 1977 proposed a modified Forman equation which includes a correction for R-ratio effects. The modified Forman equation is then

$$\frac{da}{dN} = \frac{\lambda^m C\Delta K^n}{K_{Ic} - \lambda\Delta K} \tag{19}$$

where $\lambda = 1/(1 - R)$. This last modified Forman equation was used by Speidel in 1973 along with an approximation for low ΔK to obtain an equation good at all regimes of ΔK:

$$\frac{da}{dN} = \frac{C\lambda^m(\Delta K - \Delta K_o)^n}{K_{Ic} - \lambda\Delta K} \tag{20}$$

where $\Delta K_o = \Delta K_{oo}(1 - bR)$, as discussed earlier.

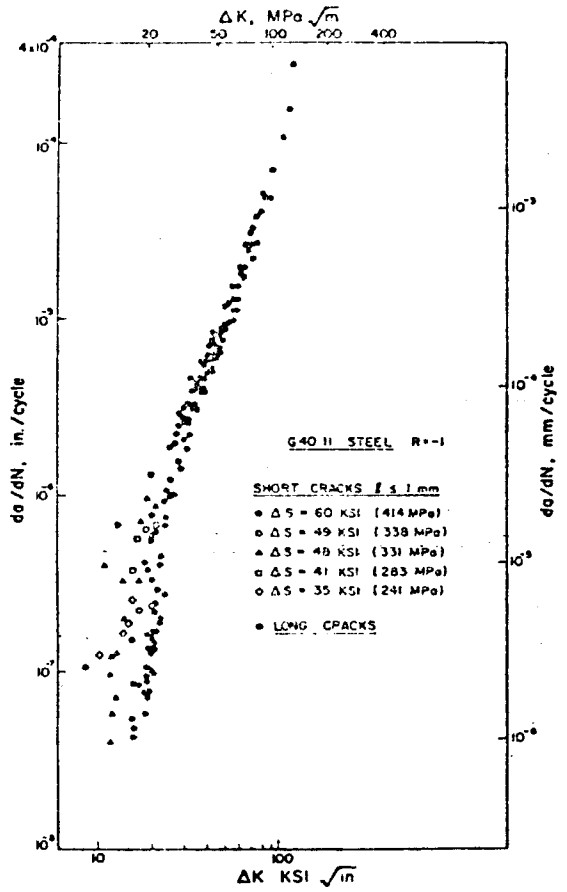

Fig. 8. Comparison of short crack with long crack results for G40.11 steel without l_o included in the ΔK solution.[23]

2.8 Temperature Effect

One final parameter must be taken into account -- temperature. There can be a marked difference in FCP rates when different temperatures are tested. In 1966 Pearson proposed[27] that da/dN for different metals can be plotted by normalizing ΔK to ΔK/E. As shown by Speidel[16] in Fig. 11, this idea works surprisingly well. Using this concept Sadananda and Shahinian[28] recognized that Young's modulus is also a function of temperature. Then, plotting da/dN

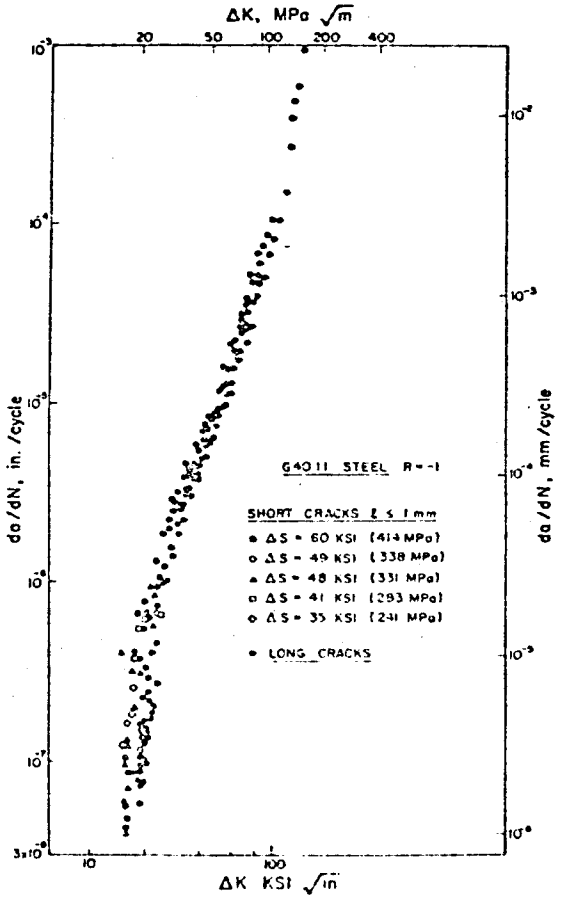

Fig. 9. Fatigue crack propagation rates as a function of ΔK.[23]

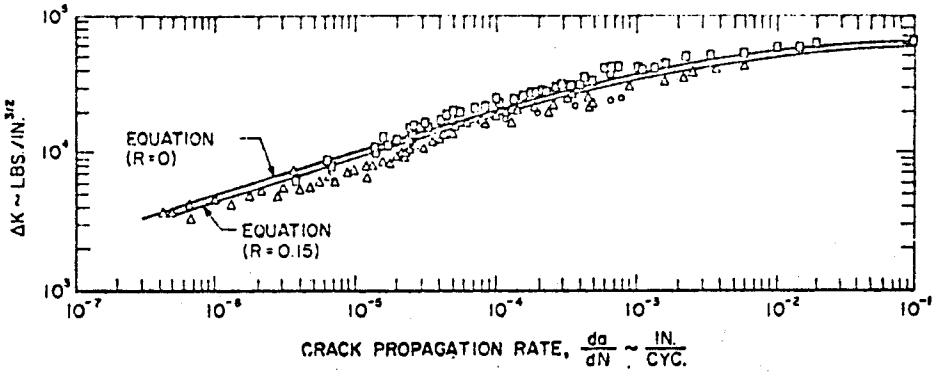

Fig. 10. Comparison of experimental and theoretical crack-propagation rates in 7075-T6 aluminum plate for R = 0 to R = 0.15.[25]

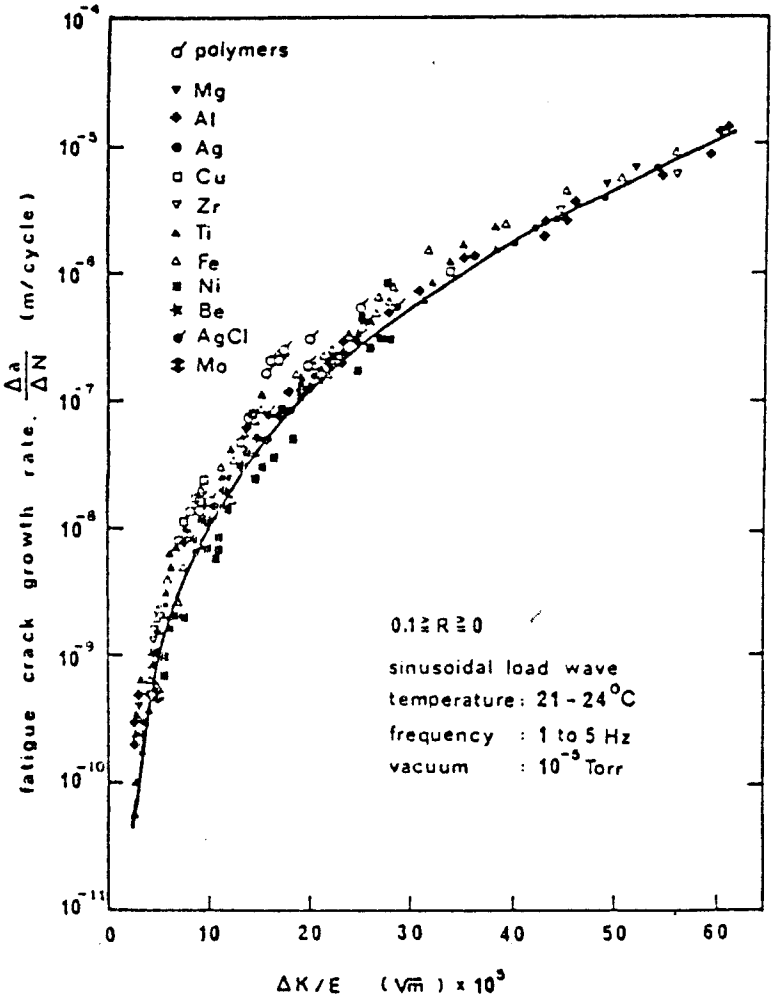

Fig. 11. Normalization of fatigue crack growth rates with Young's modulus for 11 different metals.[16]

versus ΔK/E(T), Sadananda and Shahinian showed good agreement with experimental results (see Fig. 12).

2.9 Resulting Equation

Drawing all of the above modifications together, Watson[8] in 1979 proposed the following equation to predict FCP rates

$$\frac{da}{dN} = \frac{C\lambda^m(f\Delta K - \Delta K_o)^n}{K_{Ic} - \lambda f\Delta K} \qquad (21)$$

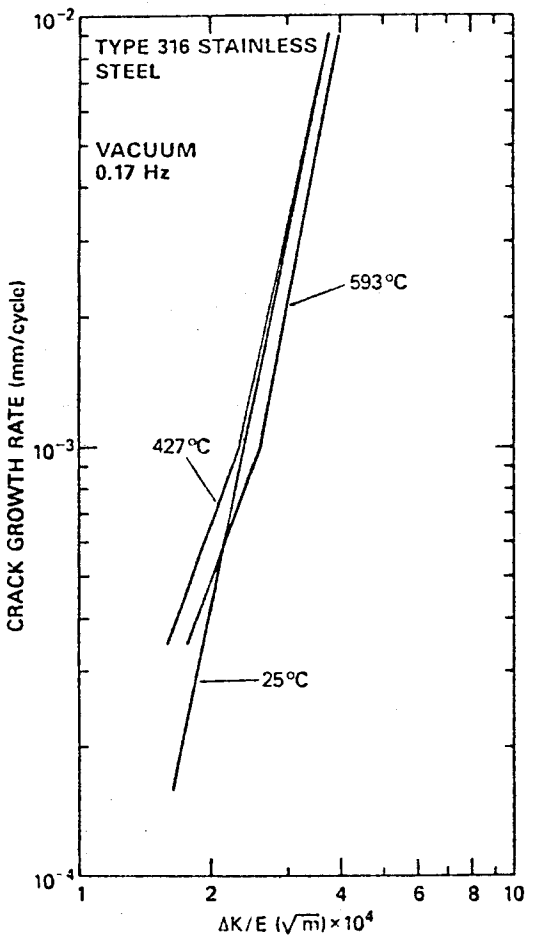

Fig. 12. Crack growth rate data in vacuum.(12)

where: $f = E(T_o)/E(T)$

E = Young's modulus

T_o = room temperature

$\lambda = 1/(1 - R)$

$\Delta K_o = \Delta K_{oo}(1 - bR)$

and C and n are fitted constants. The resulting FCP rates were calculated by Watson and are shown in Fig. 13.

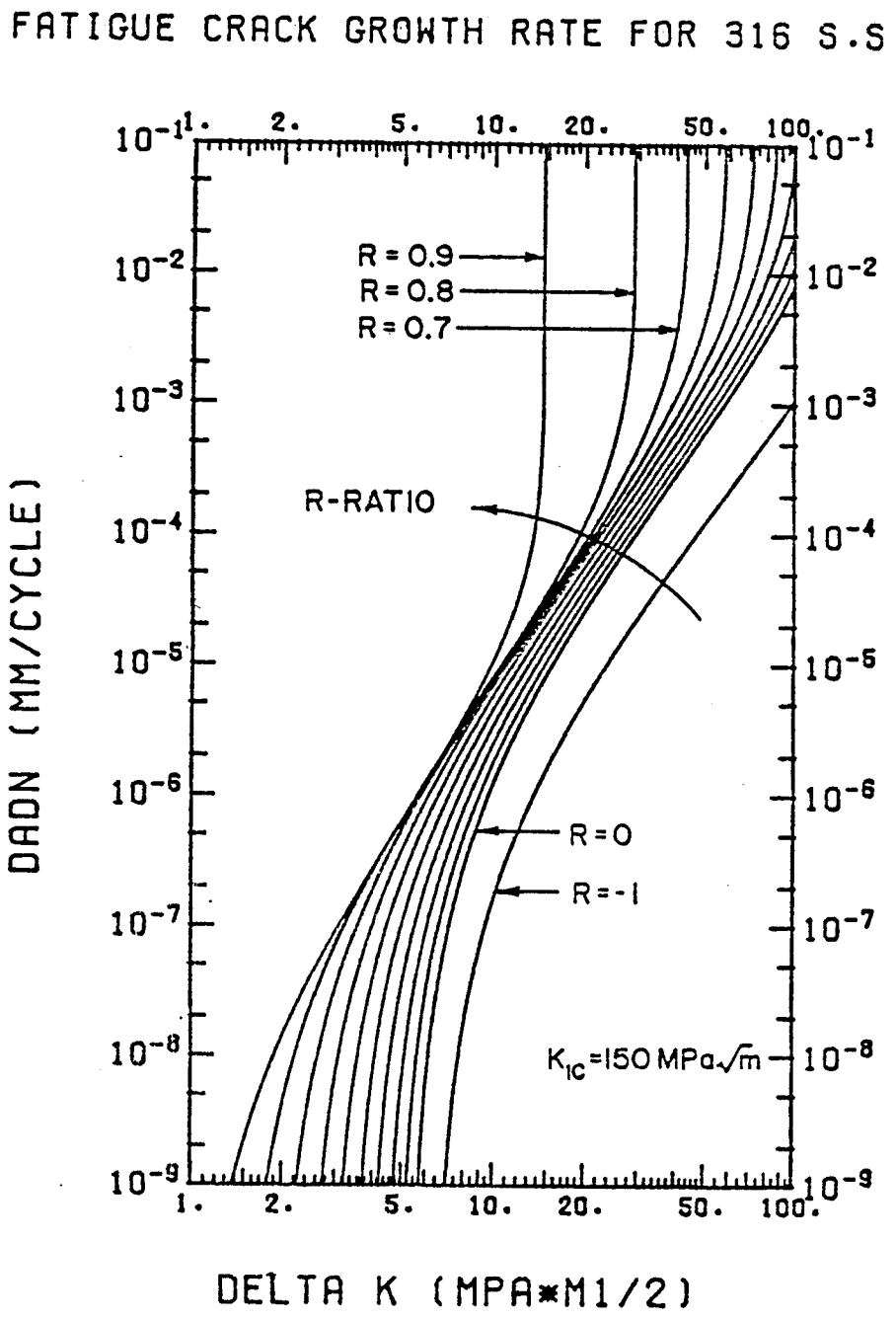

Fig. 13. Effect of R-ratio on fatigue crack growth in 316 stainless steel.[8]

2.10 Theoretical Model for FCP

Recently numerous models have been proposed for FCP. Some models relate FCP rates to Crack Opening Displacement or number of dislocations generated at the crack tip. Other models are based on the Mason-Coffin cumulative damage rule. However, the major drawback to most models is that a stress intensity threshold, ΔK_o, at which no damage occurs cannot be predicted. This author has found two relatively well-developed theoretical models for FCP near the threshold.

Lanteigne and Bailon derive[29] an expression for da/dN which predicts a threshold stress intensity, ΔK_o, and which also predicts a linear region at higher ΔK. Basically the region ahead of the crack is divided into three regions: (1) an ideal plastic region closest to the tip, (2) a work-hardening region, and (3) an elastic region. In the ideal plastic zone failure occurs according to the Mason-Coffin relationship

$$\Delta\varepsilon_p (N_f)^{\beta} = \frac{1}{2}\,\varepsilon_f' \tag{22}$$

where ε_p is the plastic strain, ε_f' is the failure strain in fatigue, N_f is the number of cycles to failure, and β is a material constant. In the work-hardening region the extent of the zone size is given by $R_m = (1/6\pi)(K/\sigma_y)^2$. In the elastic region the stress is given by $\sigma = K/(2\pi r)^{1/2}$.

To obtain a workable model in the ideal plastic region some crack radius ρ must be assumed (as it turns out ρ will be an adjustable parameter). It must also be noted that the maximum tri-axiality occurs at approximately 4ρ; the cracks should initiate at the point of maximum tri-axiality. Therefore, $da/dN = 4\rho/N_f$. After calculating the strains in the region, the FCP rate can

be given by

$$\frac{da}{dN} = \frac{4}{\rho^{(1/\beta)-1}} \left[\frac{1.3 \times 10^{-2}(\Delta K^2 - \Delta K_o^2)}{E\sigma_s \varepsilon_f'}\right]^{1/\beta} \tag{23}$$

where σ_s is the yield stress under cycling. $\Delta K_o = 12.40(\rho\sigma_s E\ \Delta\varepsilon_o)^{1/2}$, where $\Delta\varepsilon_o$ is the strain amplitude corresponding to $\Delta\sigma_o$ on a SN curve. Figure 14 shows a comparison between the above expression for da/dN and experimental results.

Radon has also developed[30] a simplified model for FCP. Basically the model assumes fatigue crack growth can occur only when the level of plastic deformation of strain ahead of the crack tip reaches the fracture strain ε_f. Assuming a work-hardenable material where n is the work-hardening exponent, the FCP rate can be given by

$$\frac{da}{dN} = \frac{2^{1+n}(1 - 2\nu)^2(\Delta K^2 - \Delta K_o^2)}{4(1 + n)\pi\sigma_{yc}^{1-n} E^{1+n} \varepsilon_f^{1+n}} . \tag{24}$$

While this result is similar to the one obtained by Lanteigne and Bailon, there is no adjustable parameter in Radon's result. Regardless, Fig. 15 shows a comparison to experimental results with remarkably good agreement.

2.11 Conclusions

While the current theoretical models are interesting, they remain questionable. However, if the threshold stress intensity, ΔK_o, is not known for a material (or an irradiated material) then the use of a theoretical model may provide an estimate for ΔK_o.

To determine actual FCP rates over the entire range of ΔK the following expression (as presented earlier) should be used

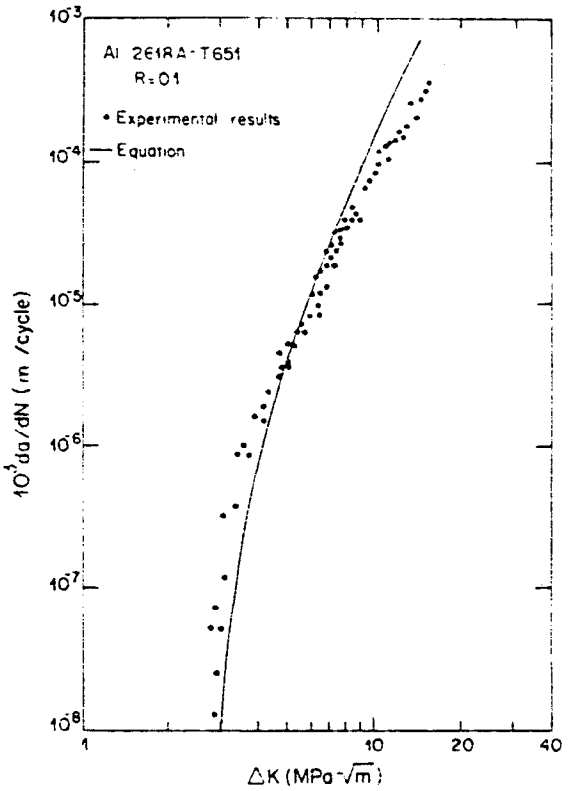

Fig. 14. Variation of fatigue crack growth rate with alternating stress intensity at R = 0.1 for Al2618A-T651.[29]

$$\frac{da}{dN} = \frac{C\lambda^m (f\Delta K - \Delta K_o)^n}{K_{Ic} - \lambda f \Delta K} \quad . \tag{25}$$

The above equation is already in WISECRACK. However, the constants for ferritic steels must be determined and programmed into the code.

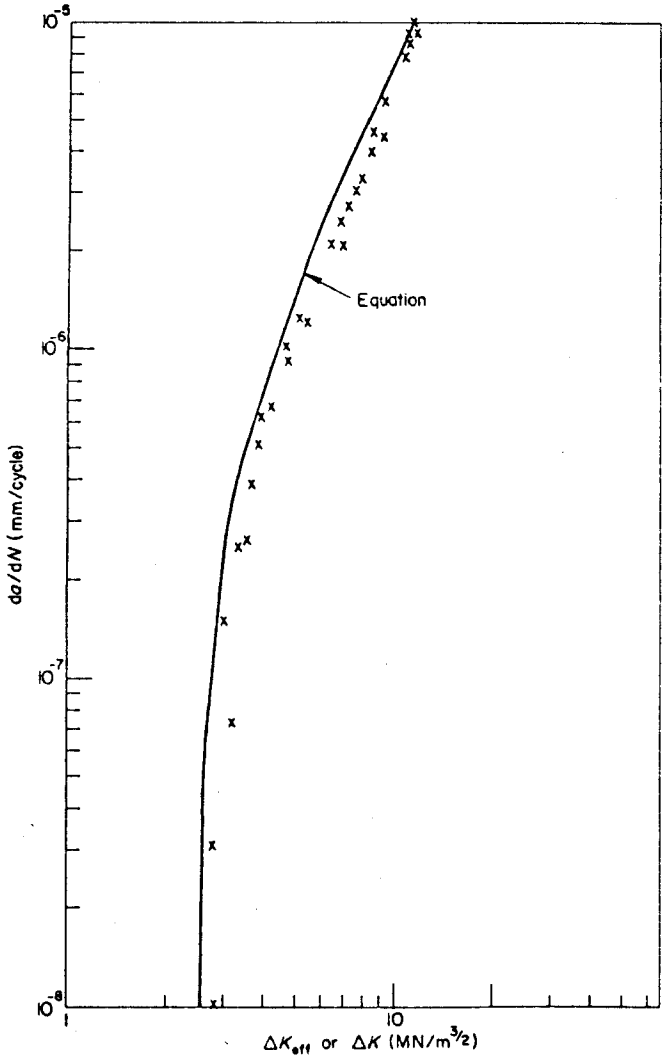

Fig. 15. da/dN vs. ΔK for BS4360-50D steel at 30 Hz in air (B = 50 mm).[30]

3. ON THE METHODS TO PREDICT CREEP CRACK GROWTH

Three different correlations to predict creep crack growth rates are examined. The linear elastic parameter K is found to be inappropriate for high temperature applications. The net section stress σ_{net} has limited applicability and seems to be restricted to plate type geometries. Finally, an elastic-plastic parameter J^* is found to correlate best with the available data. Further, creep crack growth versus J^* appears to be insensitive to temperature for the materials of interest. The value of J^* is, however, difficult to calculate. Recommendations are presented concerning prediction of creep crack growth rates for fusion reactor first walls.

3.1 Introduction

The time dependent behavior of structural materials being considered for the first generation of fusion reactors is usually characterized by creep rupture data on small scale smooth specimens. In fact, at least one author has stated[31] that creep effects in thin walled stainless steel fusion reactor blanket modules are minimal. The statement was based on results of uncracked creep rupture experiments for 316 stainless steel at 600°C for a stress of approximately 30 MPa.

To more fully predict the structural adequacy of fusion reactor components, the propagation rates of cracks (which could exist at manufacture or could develop in time) need to be better understood. While several factors influence overall crack propagation, this chapter investigates high temperature creep crack growth. Since it is anticipated that the first generation fusion reactors will use ferritic or austenitic stainless steels in the first wall or blanket modules, these alloys are highlighted as much as possible.

3.2 Theory of Creep Crack Growth

Under tensile loading conditions at high temperatures, the strain in a smooth bar increases with time until failure finally occurs. This type of time dependent deformation is called creep. A representative graph (Fig. 16) of creep strain versus time shows that the deformation is time and temperature dependent. The curve can be divided into three regions. After an initial instantaneous elastic strain, the strain rate decreases until a steady state is reached. These two regions are the transient stage and the steady state stage. Eventually, the tertiary stage of creep is reached where the strain rate increases dramatically until failure.

It has been proposed that under creep conditions the diffusion of vacancies towards a crack tip, and their condensation there, would contribute to crack growth. The growth could occur either by volume or grain boundary diffusion of vacancies toward the crack tip. This preferential diffusion is caused by a steep stress gradient which exists just ahead of the crack. A different creep crack growth model assumes that small voids nucleate and grow by diffusion ahead of the crack tip. Crack propagation is then by coalescence of the voids. There are also deformation models which attempt to relate creep crack growth to creep deformation rates. Almost all of these deformation models assume some critical criteria for crack growth, such as critical strain, critical displacement, or critical damage. Finally, there is a grain boundary sliding model which Sadananda and Shahinian present in a review paper on theoretical modeling of creep crack growth.[32] The model assumes that grain boundary sliding initiates the crack and contributes to crack growth.

It should be emphasized that none of the above models can accurately predict creep crack growth rates on an absolute scale. However, they all provide

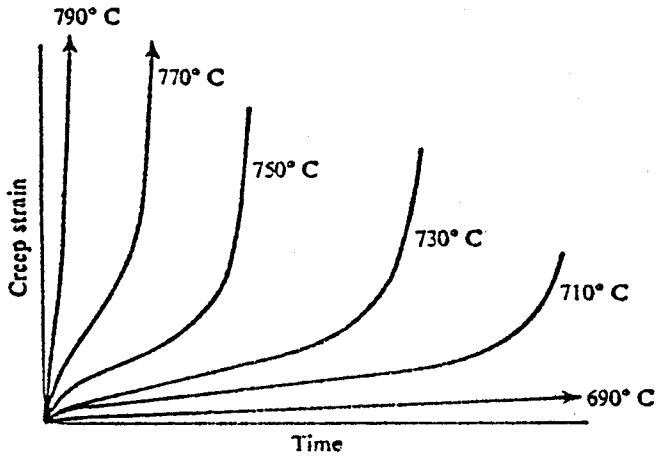

Fig. 16. Effect of varying test temperature on the creep strain curves at constant stress for a given material.[11]

a basis for understanding the many factors that could influence creep crack growth.

3.3 Fracture Mechanics Considerations

Several parameters such as stress intensity factor (K), crack opening displacement (COD), COD rate, J integral, J^* integral, net section stress (σ_{net}), and reference or equivalent stress (σ_{ref}) have been used to correlate creep crack growth rate data. While the number of studies and specimen geometries is limited, the available information suggests that for structural steels three parameters, K, J^*, and σ_{ref} (or σ_{net}), may be applicable depending on materials and test conditions.[33]

3.3.a) Stress Intensity Factor, K. Because of the relative simplicity in applying K to crack growth rates, the use of the stress intensity factor is quite appealing. However, it must be remembered that K is the parameter of interest in Linear Elastic Fracture Mechanics (LEFM). Once plasticity effects

become significant at higher temperatures and stresses, the use of LEFM (and K) becomes limited. This may be illustrated in the following way.[34] Figure 17 shows a sketch of the deformation zones ahead of a crack tip. When sufficient loading is applied, a plastic zone is formed at the crack tip. The size of the plastic zone can be characterized by K and the yield strength, σ_y, (size ~ $(K/\sigma_y)^2$). Another zone (K-zone) can be thought of as that zone ahead of the crack tip where the elastic stress and deformation field equations apply. If the plastic zone size becomes comparable to the K-zone size, K is no longer applicable. In this case stresses and strains can be characterized by another parameter J (to be discussed later). Under creep conditions the initially high stresses near the crack tip relax to a lower value. The zone where this occurs is called the creep zone. Similarly, if the creep zone becomes comparable to the K-zone, J is no longer applicable, in which case σ_{net} (or σ_{ref}) (to be discussed later) becomes a better parameter to characterize creep crack propagation rates.

Using the above illustration, it can be seen that in creep resistant materials which have a small $(K/\sigma_y)^2$, K could be the appropriate parameter to characterize creep crack growth rates.

3.3.b) J^* Integral, J^*. Introduced by Rice in 1968, J can be thought of as

$$J = -\left(\frac{1}{B}\right)\left(\frac{dU}{da}\right)_{\delta} \tag{26}$$

where B is the specimen thickness and the differential corresponds to the change in strain energy U due to an infinitesimal change in crack length at a given crack displacement δ. In a like manner, J^* is

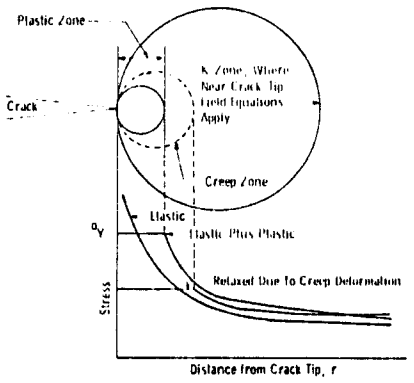

Fig. 17. Schematic representation of the deformation zones ahead of the crack tip at elevated temperatures.[34]

$$J^* = -\left(\frac{1}{B}\right)\left(\frac{d\dot{U}}{da}\right)_{\dot{\delta}} \tag{27}$$

where the dot corresponds to the time derivative. In the literature, different terms for J^* have been used. These include C^*, modified J-integral and creep J-integral.

The J^* parameter is a path independent energy rate line integral given by

$$J^* = \left(\frac{1}{B}\right) \int_{\Gamma} W^* \, dy - T_i \left(\frac{\partial \dot{u}_i}{\partial x}\right) ds \tag{28}$$

where

$$W^* = \int_0^{\dot{\varepsilon}_{mn}} \sigma_{ij} \, d\dot{\varepsilon}_{ij} \, . \tag{29}$$

As shown in Fig. 18, Γ is the line contour taken from the lower crack surface counterclockwise to the upper crack surface. W^* is the strain energy rate associated with σ_{ij} and $\dot{\varepsilon}_{ij}$. T_i is the traction vector where $T_i = \sigma_{ij} \cdot n_j$ and

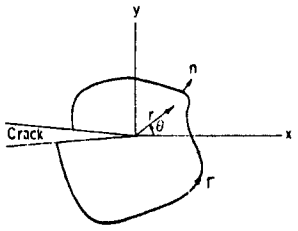

Fig. 18. Line contour around a crack.[34]

n_j is the unit outward normal. The displacement vector is u_i and s is the arc length along the contour.

The determination of J^* is nontrivial. Experimental determination of J^* requires: (1) measurement of crack length and displacement as a function of time for different loads. Then a step-by-step reduction of the data is required to obtain: (2) displacement rate versus crack length for different loads, (3) load versus displacement rate for different crack sizes, (4) strain energy rate versus crack length for different displacement rates, (5) crack growth versus displacement rate, and finally, (6) crack growth rate versus J^*. Theoretical calculations of J^* for specific geometries are quite involved. All of the models assume a creep law of the form $\dot{\varepsilon} \propto \sigma^n$, and consider only one specific specimen geometry at a time. As an example of one theoretical model, Musicco[35] has obtained for a tension specimen configuration:

$$J^* = - \frac{(n - 1)P\dot{\Delta}}{(n + 1)} \frac{1}{Bwm} \frac{dm}{d(a/w)} \tag{30}$$

where P and $\dot{\Delta}$ are the load and load point displacement rates; B, w, and a are

thickness, width, and crack length; n is the material constant used in $\dot{\varepsilon} \propto \sigma^n$, and m (a function of a/w) is the ratio of the load to produce yielding in a cracked specimen to the load to produce yielding in an uncracked specimen of the same shape. The values for m can be calculated analytically by slip line field theory. $\dot{\Delta}$ for a double cracked or central cracked tension specimen can be given by $\dot{\Delta} = b(P/bB)^n$ where $b = (b - a)$. Expressions for J^* for selected geometries can be found in the literature (see Ref. 33 for a short table of J^* values).

3.3.c) Net Section Stress (σ_{net}) or Reference Stress (σ_{ref}). As discussed earlier, when the creep zone becomes comparable to the K-zone neither J (or J^*) nor K are adequate to describe creep crack growth. The reason for this is that creep occurs so rapidly that the stresses are relaxed at a faster rate than the increase of stress due to crack growth. In the limit of extremely rapid creep, the stresses become essentially homogeneous. In this case the specimen can be thought of as behaving like uncracked creep rupture specimens with a cross-section of constant stress. A reference stress, σ_{ref}, for a cracked component is defined as that constant stress which when applied to an uncracked uniform component will give the same displacement rate. For plane strain

$$\sigma_{ref} = \frac{P}{mBw} \tag{31}$$

where P is the applied load, B is the thickness, w is the width, and m is (as defined earlier) the ratio of the load to produce yielding in a cracked body to the load to produce yielding in an uncracked body of the same shape. Values for m can be calculated (see Ref. 33 for a short table of m values).

Net section stress (σ_{net}) is defined as that constant stress which exists over the remaining uncracked section of the specimen as the result of some externally applied load. While it is expected that σ_{ref} could be a more appropriate parameter than σ_{net},[33] this author could not find sufficient experimental results to adequately justify the use of σ_{ref}. However, there is a multitude of experimental evidence which suggests that under certain geometric restrictions σ_{net} can be used.

In summary, there are three main parameters of interest in creep crack growth: K, J^*, and σ_{net} (or σ_{ref}). Which of these three is applicable to a situation depends (theoretically) on the K-zone size, the plastic zone size, and the creep zone size. These zone sizes, however, are not conveniently or accurately obtainable. [There are order of magnitude estimates which can be made for the different zone sizes. The K-zone is on the order of the specimen dimensions; the plastic zone is on the order of $(K/\sigma_y)^2$; and the magnitude of the creep zone can be found using a model proposed by Reidel and Rice.[36]] Fortunately, the validity of the parameters can be assessed by determining if creep crack growth rates are independent of the choice of crack and specimen geometry.

3.4 Results of Experiments

In 1975 Nicholson and Formby[37] correlated creep crack growth rates with net section stress, σ_{net}. Prior to this time, attempts were made to correlate limited creep crack propagation data with the stress intensity factor K. It was recognized, however, that K is not in general applicable when LEFM is not applicable. Nicholson and Formby tested type 316 stainless steel in air at 740°C. Two types of specimens were used: single edge notched (SEN) and notched center hole (NCH). The results of their tests are shown in Figs. 19

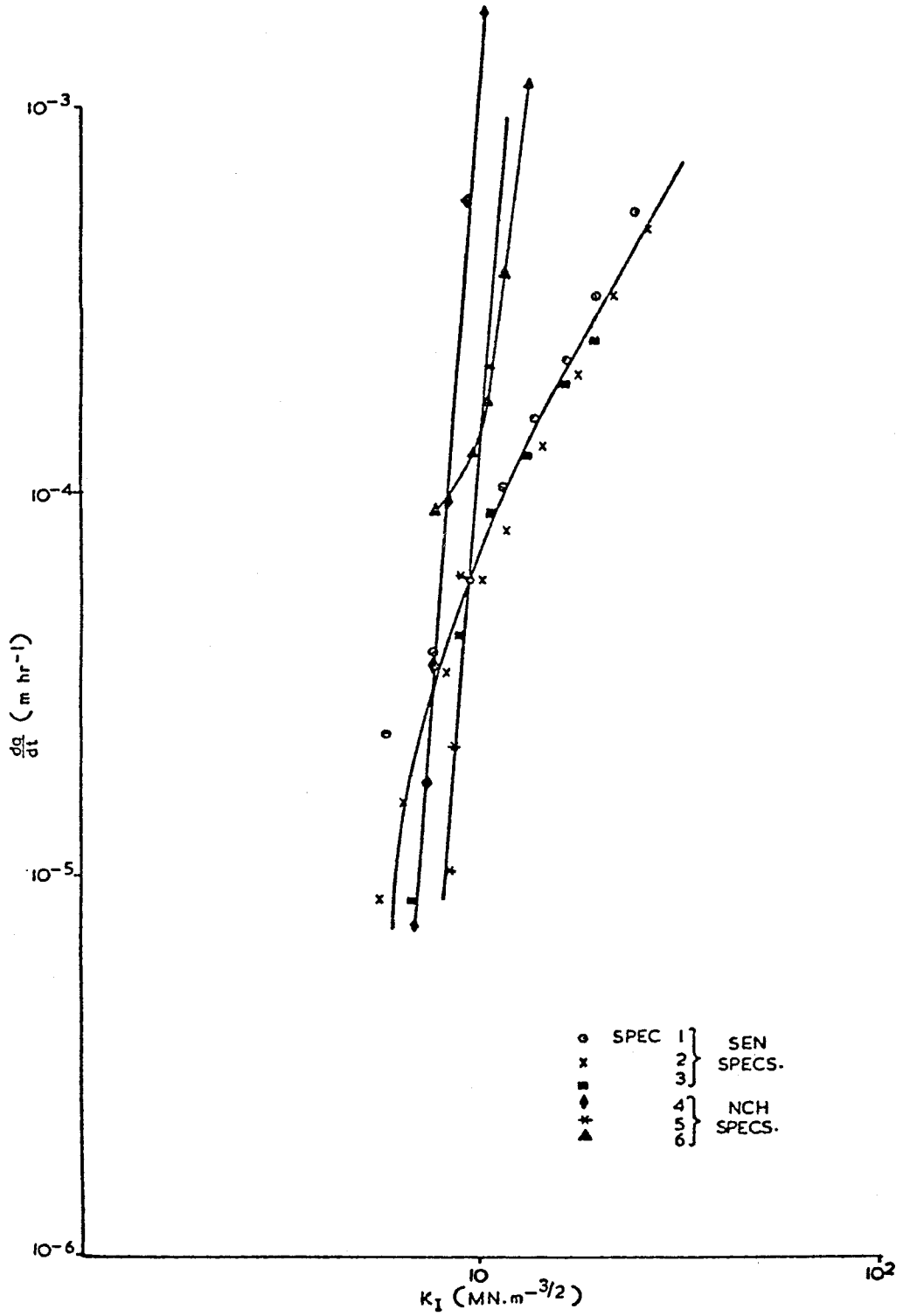

Fig. 19. Creep crack growth rate (da/dt) versus stress intensity factor (K_i).[37]

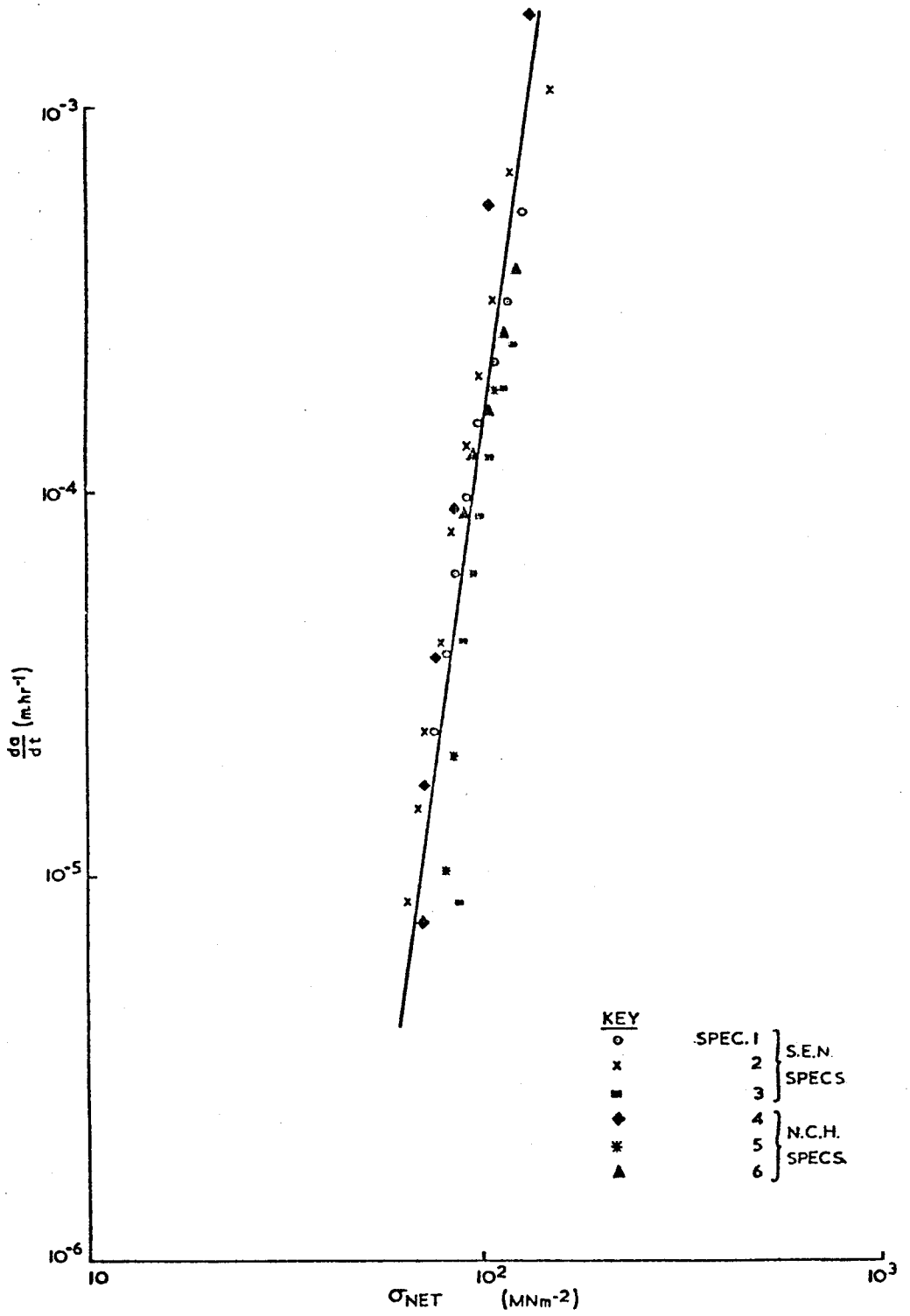

Fig. 20. Creep crack growth rate (da/dt) versus net section stress (σ_{net}).(37)

and 20. Figure 19 shows crack growth rates versus stress intensity factor. It is obvious from the plot that crack growth rate versus stress intensity factor depends on crack geometry (note at high crack growth rates the difference in value and slope of SEN and NCH specimens). The same creep crack growth rates were then plotted versus σ_{net} (Fig. 20). The growth rate versus σ_{net} is almost independent of the crack geometries. Nicholson and Formby found that their data fit the following expression quite well

$$\frac{da}{dt} = C\sigma_{net}^{n} \tag{32}$$

where da/dt is the crack growth rate, C is approximately 1.8×10^{-18}, and n is approximately 7 (units are given on the graph). In order to attempt to explain why σ_{net} is more applicable than K, Nicholson and Formby derived an expression for the time required to relax the initially high stress near the crack tip to a value of 1.5 $\sigma_{applied}$. This relaxation in the stress is due to creep relaxation. Using material properties for 316 stainless steel at 740°C, they found that the time to relax the stress is approximately 6 seconds. Considering the short time to relax stress ahead of a crack, it can be argued that the stress intensity factor should not be used to calculate stresses; rather, the stresses are nearly homogeneous and, therefore, σ_{net} should be used.

Figures 21 and 22 show the results of Jones and Tetelman.[38] Their experiments were done on type 304 stainless steel using three different crack geometries as indicated in the figures. As can be seen in Fig. 21, crack growth versus K is dependent on the crack geometry, whereas, crack growth versus σ_{net} is nearly crack geometry independent (Fig. 22). Additionally,

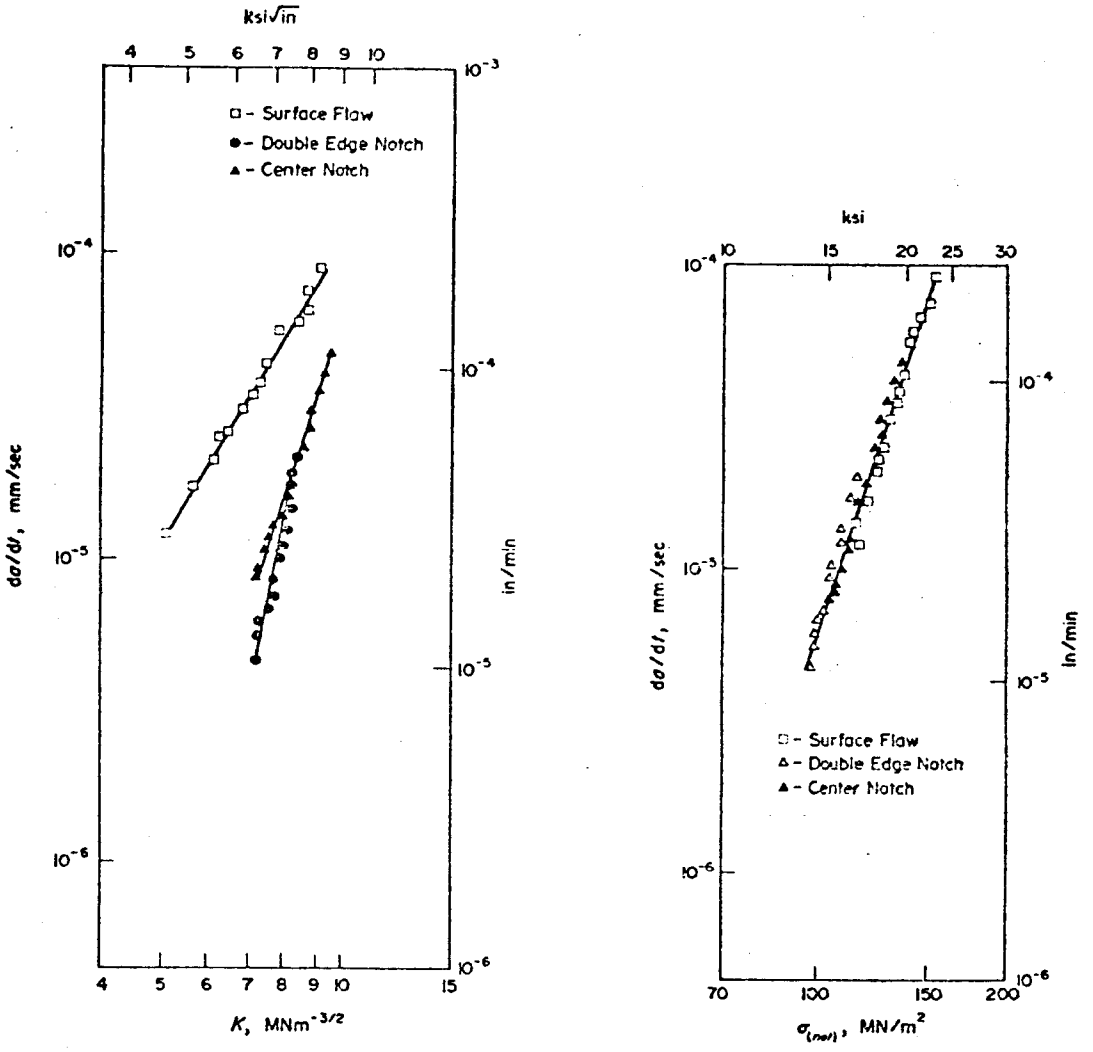

Fig. 21. Creep crack growth rate versus stress intensity factor as a function of specimen geometry.(38)

Fig. 22. Creep crack growth rate versus net section stress as a function of specimen geometry.(38)

Jones and Tetelman performed creep crack growth experiments over the range of 600 to 800°C and plotted creep crack growth rate versus σ_{net}. The results are shown in Fig. 23. They found that their results correlated well with the

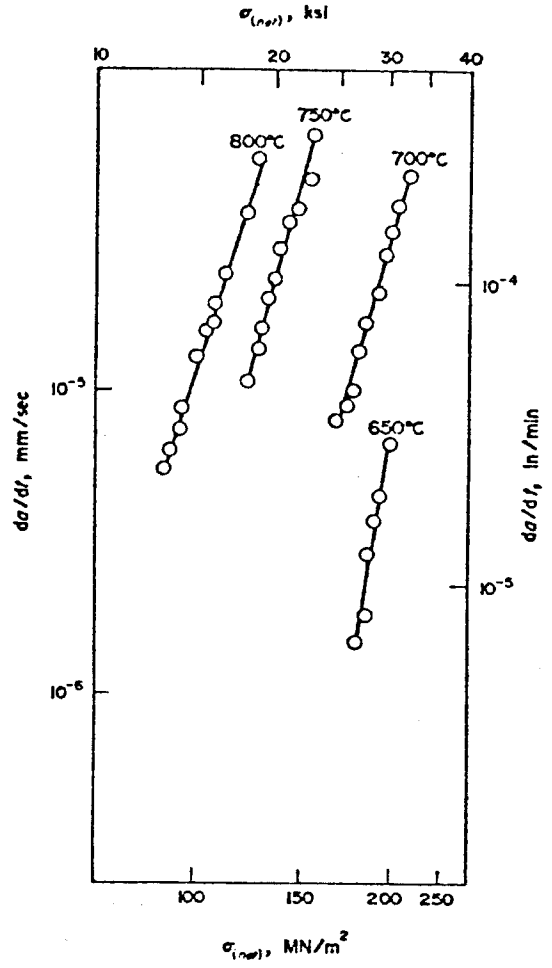

Fig. 23. Creep crack growth rate versus net section stress as a function of temperature.[38]

equation

$$\frac{da}{dt} = C\sigma_{net}^{n} \tag{33}$$

where the constants C and n are given below.

Temperature, °C	C	n
650	1.37×10^{-35}	12.9
700	1.58×10^{-21}	7.1
750	2.43×10^{-20}	7.0
800	2.07×10^{-17}	6.0

Further, a comparison was made to the exponent derived from creep rupture data where $\dot{\varepsilon} \propto \sigma^n$. The comparison is given below.

Creep Crack Growth Data		Creep Rupture Data	
T(°C)	n	T(°C)	n
		600	12.5
650	12.0		
700	7.0	700	6.6 to 8.2
750	7.1	750	6.8 to 7.2
800	6.0	800	5.9 to 6.3

Consistent with the results of Nicholson and Formby, Jones and Tetelman concluded that (for their experimental conditions) creep crack growth as a function of σ_{net} is nearly independent of geometry, which implies that σ_{net} is the parameter of interest rather than K. It was also shown that the exponent n, derived from creep rupture tests, is nearly equal to a different exponent n derived from the data of creep crack growth tests when the data is fit to an equation of the form $da/dt = C\sigma_{net}^n$. Once again the data indicate that creep crack growth rates depend on the net section stress much like creep rates (in creep rupture) depends on applied stresses. In other words, the creep crack

growth rate is proportional to the creep rate in the uncracked ligament ahead of the crack tip.

Thus far in this paper the results of creep crack growth rate tests have been reported for several crack geometries (SEN, NCH, etc.). It has been shown that the results of creep crack growth correlate well with net section stress σ_{net}. However, all the specimen geometries discussed were flat plate type specimens. Taira, Ohtani and Kitamura performed creep crack growth tests[39] on type 304 stainless steel and on low carbon steel using flat plate geometries and also cylindrical geometries. The cylindrical geometries included thin walled center notched cylinders (CNC) and round notched bars (RNB). They found that creep crack propagation rate versus net section stress σ_{net} is clearly a function of geometry for CNC and RNB specimens (see Fig. 24). It must be noted that the test was done at 400°C, a lower temperature than all other tests previously reported herein. While Taira et al. do not discuss how rapid stress relaxation is at this lower temperature, it is possible that stresses are not essentially homogeneous as Nicholson and Formby concluded at a higher temperature.[37] It should be recalled that rapid stress relaxation resulting in homogeneous stresses is the basis for using the σ_{net} parameter to characterize creep crack growth rates. If it can be assumed that creep relaxation is not significant enough, then it should not be surprising that σ_{net} does not characterize this creep crack growth. Taira et al. then characterized creep crack growth rates as a function of J^* (which they call creep J-integral or J). The results are shown in Fig. 25. It is clear that in their case J^* correlates quite well with the crack growth rate and is nearly independent of geometry. Additionally, Taira et al. plotted crack propagation rate versus σ_{net} and versus J^* for 400 and 500°C (Figs. 26 and 27). It

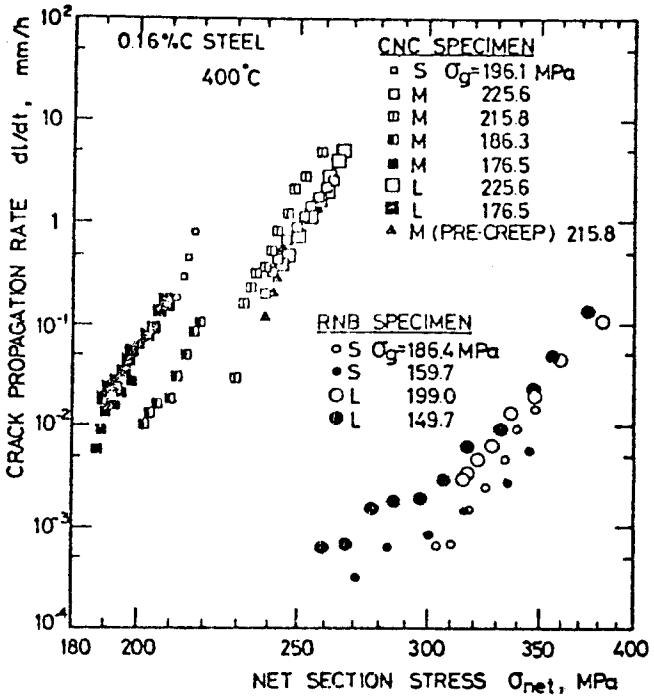

Fig. 24. dl/dt versus σ_{net} for CNC-L, M, and S specimens and RNB-L and S specimens at 0.16% carbon steel at 400°C.[39]

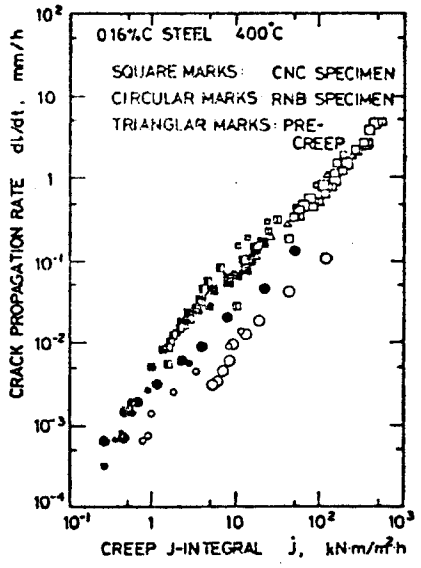

Fig. 25. dl/dt versus $\dot{J}$ for the same test results with those in Fig. 24.[39]

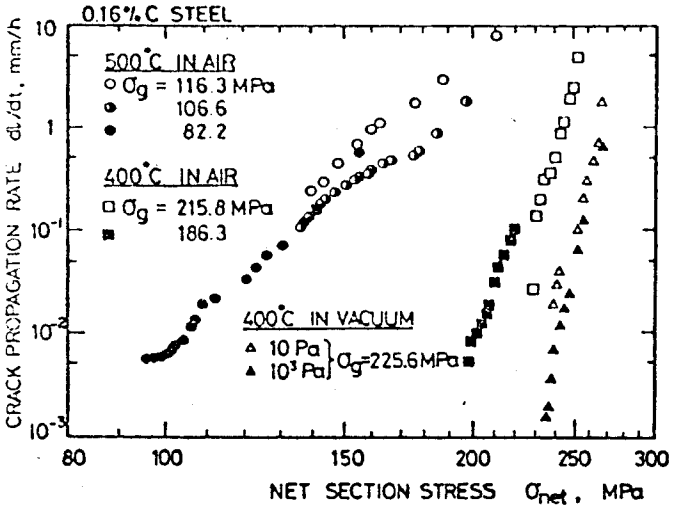

Fig. 26. dl/dt versus σ_{net} for CNC-M specimens of 0.16% carbon steel at 400 and 500°C in air and at 400°C in vacuum.(39)

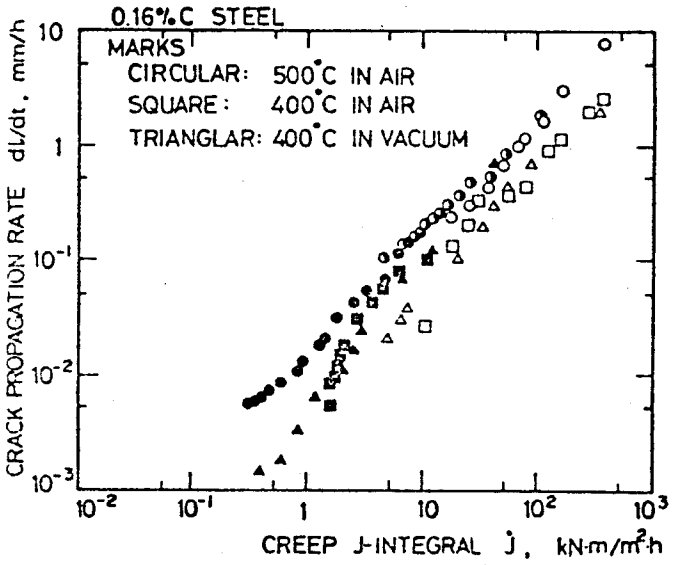

Fig. 27. dl/dt versus $\dot{J}$ for the same test results with those in Fig. 26.(39)

is seen in Fig. 26 that there is quite a difference in correlation between 400 and 500°C data. However, in Fig. 27 the data as a function of J^* is nearly independent of temperature. Two other plots of crack propagation rate versus J^* were given by Taira et al. (Figs. 28 and 29). While they noted the good correlation between crack growth and J^*, one point was not mentioned by them: crack growth versus J^* plots are nearly independent of temperature for the steels tested (0.16% C steel at 400 and 500°C, 316 stainless steel at 600 and 650°C, and 304 stainless steel at 650°C). This can be seen by comparing Figs. 25, 27, 28, and 29.

The apparent temperature insensitivity of the crack growth versus J^* of one of these steels, type 304 stainless steel, was further investigated by Saxena.[34] His results are shown in Fig. 30. This figure indicates that for 304 stainless steel in the temperature range of 538-705°C, the creep crack growth rate versus J^* (C^* in Saxena's paper) is not very sensitive to temperature. Also, Sadananda and Shahinian postulate, based on data accumulated (see Fig. 31),[33] that there may be a unique da/dt - J^* relationship for some steels independent of material and temperature.

3.5 Conclusions

The stress intensity factor K was not found to correlate well with creep crack propagation rates for the experiments discussed above. However, as Sadananda and Shahinian point out,[33] for materials that are significantly sensitive to the environment the linear elastic parameter K may adequately characterize crack growth. Further, for high strength creep resistant alloys, LEFM (and consequently K) may apply.

For the case of first wall fusion reactor material, which is anticipated to be ferritic or austenitic stainless steel operated at high temperatures, K

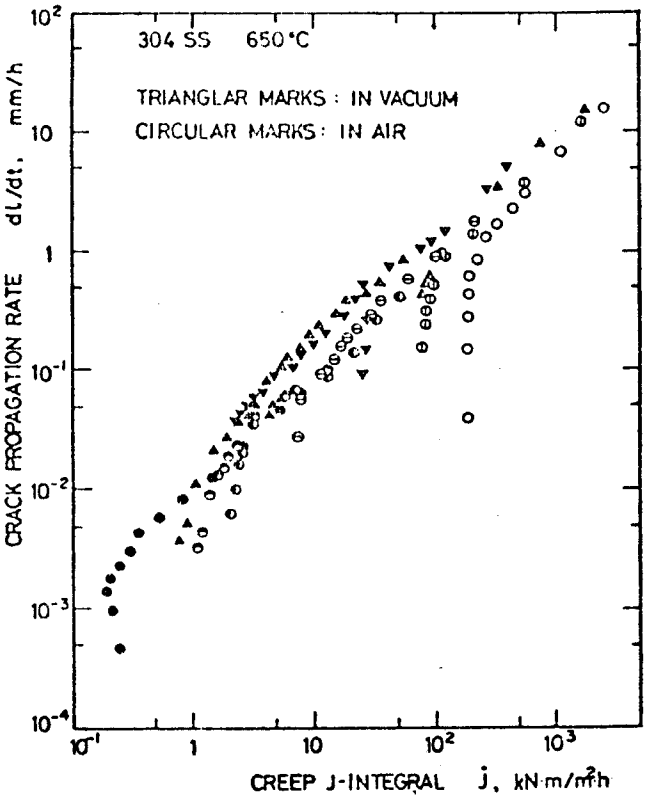

Fig. 28. dl/dt versus $\dot{J}$.(39)

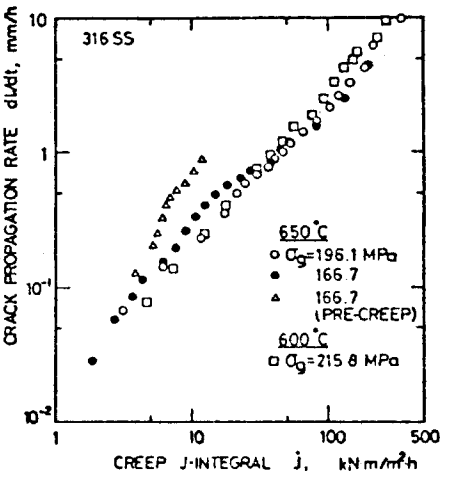

Fig. 29. dl/dt versus $\dot{J}$ for CNC-M specimens of type 316 stainless steel at 600 and 650°C.(39)

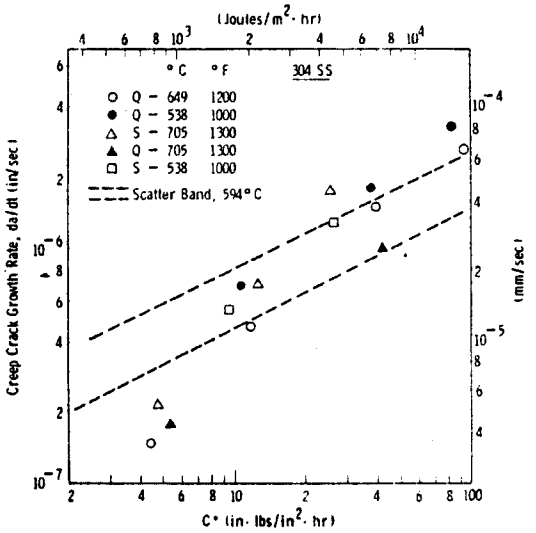

Fig. 30. Creep crack growth rate as a function of temperature and heat treatment for 304 stainless steel. "S" refers to sensitized treatment and "Q" refers to an "as quenched condition."[34]

is probably not the parameter of interest. However, some designs specify a lead/lithium liquid metal coolant in contact with the walls. If this coolant severely affects creep crack growth rates, then K may be appropriate. In this regard Krompholz, Huthmann, Grosser, and Pierick have performed (on type 304 stainless steel) creep crack growth rate experiments in air and in liquid sodium. Krompholz et al. found[40] no difference between the creep crack growth rates in air and in sodium. No data, however, is available for crack growth rates in lead/lithium. As a first approximation, one could assume that lead/lithium will not severely affect creep crack growth rates.

J^* has been shown to correlate well with creep crack growth in the previously discussed experiments. However, the creep rate in the first wall structure may be so high that stresses relax very quickly; in this case σ_{net} may be the parameter of interest.

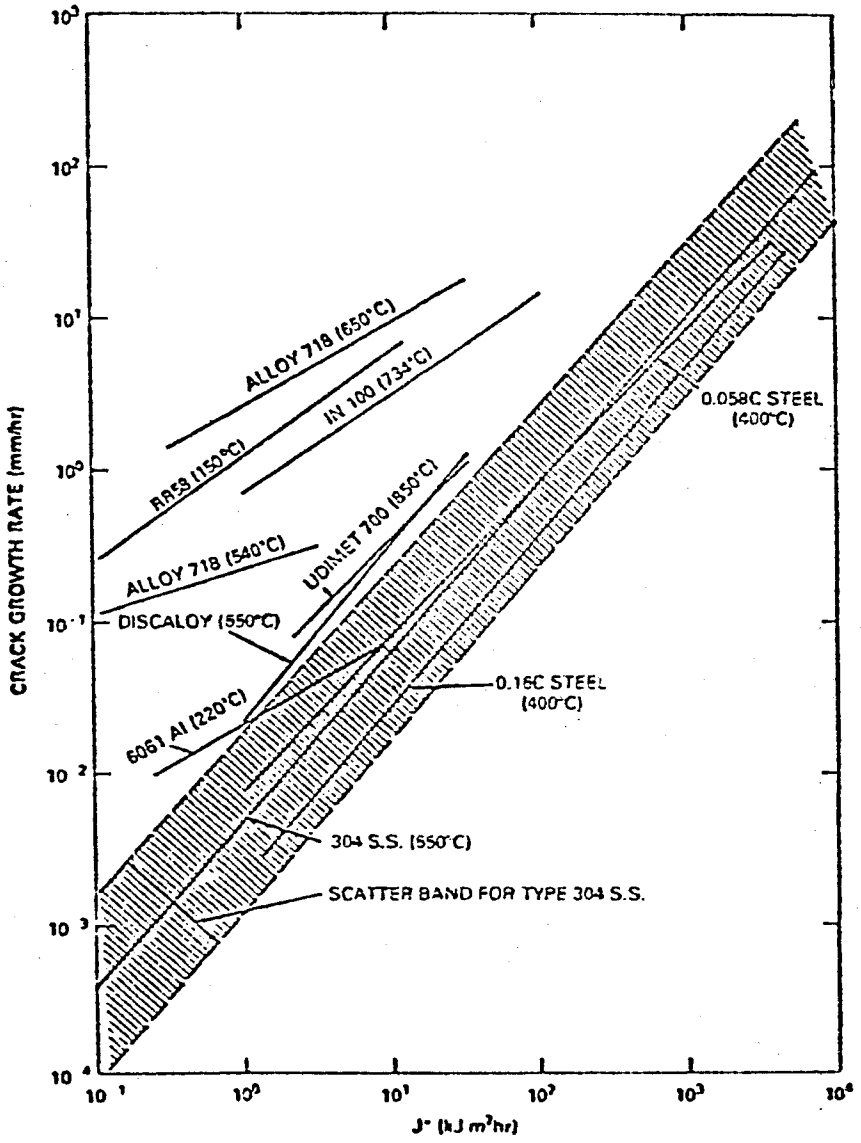

Fig. 31. Creep crack growth data of several alloys in terms of J^* parameter. Data for materials that show crack growth by predominantly deformation processes fall within or close to the data band for type 304 stainless steel.(33)

This author has not found an abundance of creep crack growth data for ferritic stainless steels. Sadananda and Shahinian[33] do, however, discuss some aspects of creep crack growth for Cr-Mo-V steels. For one composition of this alloy, creep crack growth has been correlated with K and J^*. Once again J^* appears to be better than K to characterize creep crack growth. If, however, the ferritic stainless steels creep very quickly, then σ_{net} (or σ_{ref}) may be more appropriate.

The current version of WISECRACK uses a correlation with ΔK and not σ_{net} or J^*. The code will be modified as necessary to use a correlation to whichever parameter is appropriate.

4. PROPOSED FAILURE CRITERIA

A criterion for determining if failure will occur is proposed. The criterion is based on the Heald, Spink and Worthington[41] model. Basically, failure will occur whenever K exceeds the linear elastic parameter K_{Ic} or when the stress exceeds the collapse stress as determined by plasticity theory.

4.1 Introduction

In the last few decades increasing attention has been paid to failure analysis, particularly with emphasis to fracture mechanics. Several failure assessment criteria have been proposed including: (1) K_{Ic}, (2) J-integral, (3) Crack Opening Displacement (COD), (4) R-curve, (5) Von Mises or Tresca yield criterion. Several of these criteria are reviewed by Larsson.[42] The J-integral, COD, and R-curve are either analytically difficult in a general case or are based mostly on empirical studies. K_{Ic} is a valid failure criterion; but, it is only useful for brittle materials in a plane strain state of stress. Von Mises or Tresca yield criteria are valid for fully plastic behavior, but only for smooth uncracked specimens.

From an engineering viewpoint, a failure criterion should be valid over a wide range of conditions (brittle-plastic, plane stress-plane strain) and should be computationally as simple as possible. From the brief discussion above, it seems that the union of K_{Ic} and Von Mises or Tresca criteria would meet these conditions at the extremes of brittle and ductile behavior, respectively.

The computer code WISECRACK which has been used by Watson[8] considered failure to occur when either the crack propagated through the wall (leak-through) or when the stress intensity factor K exceeded the plane strain frac-

ture toughness K_{Ic}. The failure criterion currently in WISECRACK is not entirely appropriate. Firstly, since the first wall is expected to be rather thin (~ 10 mm, i.e., plane stress), the use of the plane strain fracture toughness is not appropriate, although it is conservative. Secondly, failure by plastic collapse was not modeled. Hence, one possibly significant failure mode was ignored. The proposed failure criteria discussed below will consider plastic collapse; there are plans to incorporate a wall thickness effect on K_{Ic} into the failure criteria.

4.2 Proposed Failure Criteria Approach

In 1975 Dowling and Townley[43] proposed a two criteria approach to failure assessment of structures containing defects. The approach assumes that failure occurs when either: (1) the applied stress reaches the failure stress based on Linear Elastic Fracture Mechanics (LEFM) ($K > K_{Ic}$), or (2) the applied stress exceeds the plastic collapse stress based on plasticity theory using an appropriate yield criterion (Von Mises or Tresca yield criterion). There is, however, a sizeable transition between fully brittle and fully plastic conditions. To bridge this transition region, Dowling and Townley used the results of Heald et al. Heald et al. showed that the transition region between brittle and plastic can be described by expanding on the Bilby-Cottrell-Swinden (BCS) strip yield model.[44]

The BCS model treats a crack and the plastic zone ahead of the crack as dislocation pile-ups. Then using continuous distribution theory, the size of the plastic zone and the displacement at the crack tip can be calculated. The BCS model results are similar to the simpler Dugdale model[45] for the spread of plasticity, as expanded by Burdekin and Stone.[46]

The Dugdale model assumes a crack of length 2a normal to an applied stress σ_{app}. Plastic yielding takes place over a length dy = c - a ahead of the crack tip (see Fig. 32). The size of the plastic zone dy can be calculated by assuming a uniform stress σ_{app} over a crack of length 2c where $K = \sigma_{app}(\pi c)^{1/2}$ and then assuming a stress equal to the yield stress σ_y applied over a length c - a. It can be shown that under these conditions $K = 2\sigma_y(c/\pi)^{1/2} \cos^{-1}(a/c)$. By conservation laws, the two expressions for K can be set equal to each other; one obtains

$$\frac{a}{c} = \cos\left(\frac{\pi\sigma_{app}}{2\sigma_y}\right) \tag{34}$$

or

$$dy = c - a = c\left[\sec\left(\frac{\pi\sigma_{app}}{2\sigma_y}\right) - 1\right] . \tag{35}$$

From the BCS model one can obtain

$$\delta = 4\sigma_y c \frac{1 - \nu}{\pi\mu} \ln\left(\frac{c}{a}\right) \tag{36}$$

where δ is the Crack Opening Displacement (COD) and μ is the shear modulus. Combining the last two equations

$$\delta_c = 4\sigma_y c \frac{1 - \nu}{\pi\mu} \ln\left\{\sec\left(\frac{\pi\sigma_f}{2\sigma_y}\right)\right\} \tag{37}$$

where σ_{app} is replaced by the failure stress σ_f and δ is replaced by the COD at failure δ_c. Rearranging the last equation

$$\sigma_f = \frac{2\sigma_y}{\pi} \sec^{-1}\left[\exp\left(\frac{\pi\mu\delta_c}{4(1 - \nu)\sigma_y c}\right)\right] \tag{38}$$

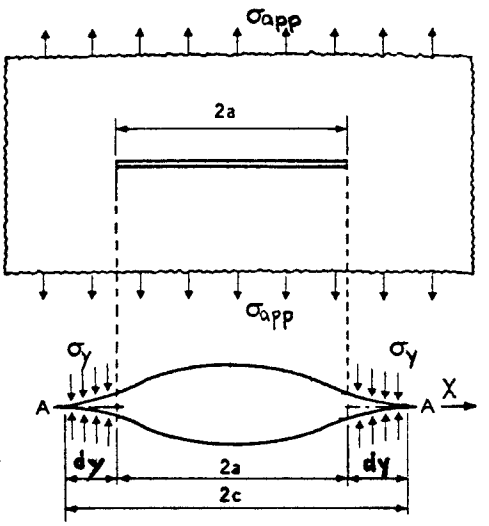

Fig. 32. Dugdale plastic strip model for infinite plate.(45)

or $$\sigma_f = \frac{2}{\pi}\,\sigma_y \cos^{-1}\left[\exp\left\{-\frac{\pi\mu\delta_c}{4(1-\nu)\sigma_y c}\right\}\right] . \qquad (39)$$

For a/c << 1 and expanding the "$\cos^{-1}$ exp" term, one obtains $\sigma_f = [(2\mu\delta_c\sigma_y)/(\pi(1-\nu)c]^{1/2} = [E(\sigma_y\delta_c)/\pi(1-n^2)c)]^{1/2} - [(E2\gamma/(\pi(1-\nu^2)c)]^{1/2}$ where 2γ is the surface energy. The last expression for σ_f is the Griffith fracture criterion for plane strain. It is reassuring to note that the complicated expression for σ_f reduces to the Griffith criterion for small plastic zone size. The Griffith fracture criterion states that $K_{Ic} = [E\sigma_y\delta_c/(1-\nu^2)]^{1/2}$. Solving for δ_c yields

$$\delta_c = \frac{K_{Ic}^2(1-\nu^2)}{E\sigma_y} = \frac{K_{Ic}^2(1-\nu)}{\sigma_y 2\mu} . \qquad (40)$$

Now back substituting gives

$$\sigma_f = \frac{2}{\pi} \sigma_u \cos^{-1}\left[\exp\left\{-\left(\frac{\pi K_{Ic}^2}{8\sigma_u^2 c}\right)\right\}\right] \tag{41}$$

where the ultimate stress σ_u has replaced σ_y since σ_u is a better measure of failure than σ_y. The above expression for σ_f is the same as that derived by Heald et al. It is interesting to note that in the limit of large K_I, $\sigma_f = \sigma_u$; and in the limit of small K_{Ic}, $\sigma_f = K_{Ic}/(\pi c)^{1/2}$.

In order to describe the failure of more complex structures the above formula can be rewritten as

$$\frac{L_f}{L_u} = \frac{2}{\pi} \cos^{-1}\left[\exp\left\{-\left(\frac{\pi^2 L_k^2}{8L_u^2}\right)\right\}\right] \tag{42}$$

where L_f is the failure load, L_u is the plastic collapse load, and L_k is the LEFM load limit. Figure 33 shows a plot of the above relationship along with some data points determined by Dowling and Townley.

While the above expression can be used to predict if failure will occur at a given load L (L replaces L_f), Harrison, Milne, and Loosemore in 1980 rewrote the expression[47] as

$$K_r = S_r \left\{\frac{8}{\pi^2} \ln \sec\left(\frac{\pi}{2} S_r\right)\right\}^{-1/2} \tag{43}$$

where: K_r = stress intensity factor/fracture toughness and

S_r = applied load/collapse load.

Figure 34 shows a plot of K_r versus S_r. The diagram is called the Failure Assessment Diagram. For a given structure with a given load, a point can be found on Fig. 34. If the point is within the curve failure is avoided.

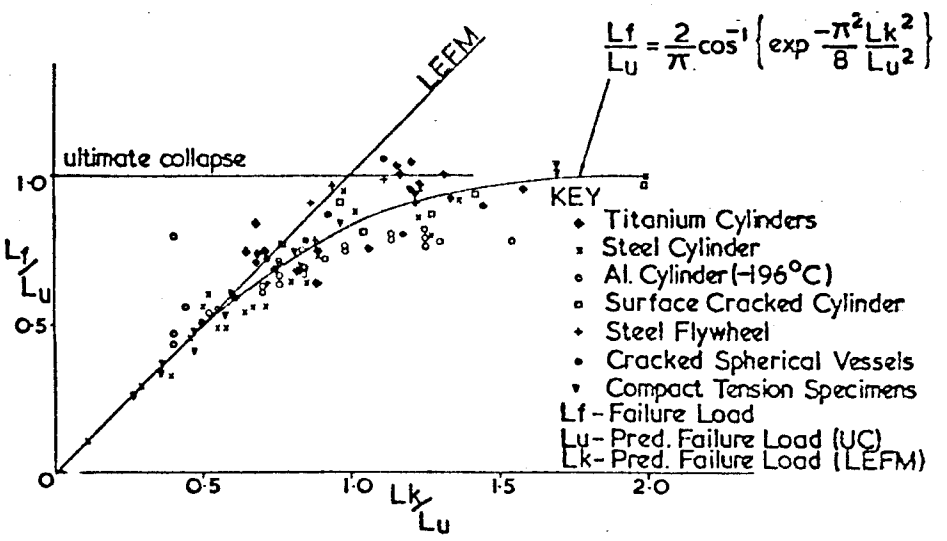

Fig. 33. Universal failure curve.[43]

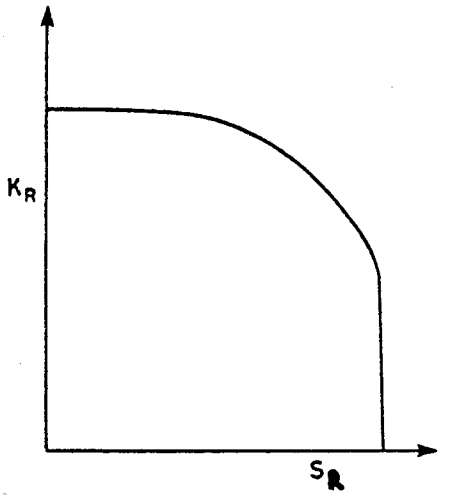

Fig. 34. Failure assessment diagram.[47]

The Failure Assessment Diagram is the cornerstone of the Failure Assessment Route R-6 as outlined by Harrison et al.

4.3 Method of Solution

The basic procedure for solution discussed herein was proposed by Harrison et al. and outlined[48] by Darlaston. The procedure consists of the following items to be evaluated at each point in time:

a) determine flaw shape and specimen geometry;

b) determine the stresses at the flaw location;

c) calculate stress intensity factor K_{Ic};

d) determine the collapse load for the specimen;

e) calculate K_r and S_r;

f) determine where on the Failure Assessment Diagram the point appears;

g) determine if the flaw is acceptable (for no-failure the point must lie within the curve).

4.4 Conclusions

A procedure for determining the acceptability of a flaw has been presented. The procedure is based on models by Bilby et al. and Dugdale, and by Heald et al. Harrison et al. first proposed the procedure in 1977. To determine the acceptability of a structure with a flaw, first graph the following equation as K_r versus S_r

$$K_r = S_r \left\{\frac{8}{\pi^2} \ln \sec \left(\frac{\pi}{2} S_r\right)\right\}^{-1/2} . \qquad (44)$$

Then given the stress intensity factor and applied load, find the corresponding point on the graph. If the point is within the curve, failure is avoided.

It should be noted that the Electric Power Research Institute (EPRI) is pursuing a different means of analysis for plastic crack growth and failure criteria. Marston states[49] that the J-integral, dJ/da, and the COD appear to be the most promising parameters for determining crack growth. Experimentally determined R-curves can be used to determine if failure will occur. The EPRI approach is not being used in this research because final experimental results are not available for the R-curves.

Currently in WISECRACK, failure is assumed to occur either by leak-through or when K exceeds K_{Ic}. Improvements to the code will include: (1) adjustment of K_{Ic} to account for a thin wall (change the plane strain criterion to a plane stress criterion), and (2) the additional failure mode of plastic collapse.

5. SUMMARY

It is proposed that the doctoral research for this author involves development of a comprehensive structural analysis code to evaluate the materials and structural performance of first wall components. The program will include:

1. Revising the computer codes TSTRESS and WISECRACK to model a shell structure capable of bending, and to model ferritic stainless steel.
2. Revising the correlations for creep crack growth to more adequately model the crack growth.
3. Revising the existing failure criteria to include the effect wall thickness on fracture toughness, and to model the additional failure mode of plastic collapse.

Acknowledgment

Support for this work has been provided by the U.S. Department of Energy.

References

1. McDonnell Douglas Staff; "Fusion Reactor First Wall/Blanket Systems Tokamak Concepts," EPRI-472-1 (1977).

2. B.A. Cramer, J.W. Davis, R.C. Kinder, and D.A. Bowers, "An Approach for Determining the Lifetime of a First Wall Structure in a Tokamak Reactor," Proceedings of the Second Topical Meeting on the Technology of Controlled Nuclear Fusion, CONF-760935-P4, Richland, WA (1976).

3. G.M. Fuller et al., "Fusion Reactor First Wall/Blanket Systems Analysis of Tokamak Concepts," EPRI-ER-582 (1977).

4. W.G. Wolfer and R.D. Watson, "Structural Performance of a Graphite Blanket in Fusion Reactors," University of Wisconsin Report UWFDM-258 (1978).

5. T.V. Prevenslick, "Structural Evaluation of a Tokamak Reactor Cylindrical Module Blanket Concept," Westinghouse Report WFPS-TME-096 (1978).

6. U.S. Contribution to the International Tokamak Reactor Phase-1 Workshop: "Conceptual Design, Chapter 7, First Wall and Limiter Systems," USA INTOR/81-1 (1981).

7. "STARFIRE - A Commercial Tokamak Fusion Power Plant Study," Argonne Report ANL/FPP-80-1, Vol. 1, Chapter 10 (1980).

8. R.D. Watson, "The Impact of Inelastic Deformation, Radiation Effects, and Fatigue Damage on Fusion Reactor First Wall Lifetime," Ph.D. Thesis, University of Wisconsin-Madison (1981).

9. R.D. Watson and W.G. Wolfer, "Impact of Material Problems on Fusion Reactor Designs," SMiRT-6 Seminar, Paris, France (1981).

10. R.R. Peterson, R.D. Watson, W.G. Wolfer, and G.A. Moses, "TSTRESS - A Transient Stress Computer Code," University of Wisconsin Report UWFDM-382 (1980).

11. Babcock and Wilcox, "Steam - Its Generation and Use," 30.5-30.6 (1975).

12. P.C. Paris and F. Erdogan, "A Critical Analysis of Crack Propagation Laws," J. of Basic Engr. 85, 528-534 (1963).

13. E.K. Walker, Air Force Flight Dynamics Laboratory Report AFFDL-TR-70-144, p. 225 (1970).

14. A.M. Sullivan and T.W. Crooker, "Analysis of Fatigue Crack Growth in a High-Strength Steel," J. of Pressure Vessel Tech. (May 1976).

15. M. Klesnil and P. Lukas, "Effect of Stress Cycle Asymmetry on Fatigue Crack Growth," Mater. Science and Engr. 9, 231-240 (1972).

16. M.O. Speidel, "Fatigue Crack Growth at High Temperatures," Proceedings of the Symposium on High-Temperature Materials in Gas Turbines, Baden, Switzerland (1974), pp. 207-251.

17. R.J. Donahue, H.McI. Clark, P. Atanmo, R. Kumble, and A.J. McEvily, "Crack Opening Displacement and the Rate of Fatigue Crack Growth," Intern. J. of Fracture Mechanics 8, 209-219 (1972).

18. R.O. Ritchie, "Influence of Microstructure on Near-Threshold Fatigue Crack Propagation in Ultra-High Strength Steel," Metal Science, 368-381 (August/September 1977).

19. J.M. Barsom, "Fatigue Behavior of Pressure Vessel Steels," Welding Research Council Bulletin 197, 1-22 (1974).

20. O. Vosikovsky, "The Effect of Stress Ratio on Fatigue Crack Growth Rates in Steels," Engr. Fracture Mechanics 2, 595-602 (1979).

21. S. Pearson, "Initiation of Fatigue Cracks in Commercial Aluminum Alloys and the Subsequent Propagation in Very Short Cracks," Engr. Fracture Mechanics 7, 235-247 (1975).

22. A. Talug and K. Reifsnider, "Analysis and Investigation of Small Flaws," ASTM STP 637, 81-96 (1977).

23. M.H. El Haddad, K.N. Smith and T.H. Topper, "Fatigue Crack Propagation of Short Cracks," J. of Engr. Mater. and Tech. 101, 42-46 (1979).

24. M.H. El Haddad, T.H. Topper and K.N. Smith, "Prediction of Non-Propagating Cracks," Engr. Fracture Mechanics 11, 573-584 (1979).

25. R.G. Forman, V.E. Kearney and R.M. Engle, "Numerical Analysis of Crack Propagation in Cyclic-Loaded Structures," J. of Basic Engr., 459-464 (September 1967).

26. H. Nordberg, "The Effect of Microstructure on Fatigue Crack Growth in a 12 Percent Chromium Steel," Scandinavian J. of Metallurgy 1, 23-25 (1972).

27. S. Pearson, "Fatigue Crack Propagation," Nature 211, 1077-1078 (1966).

28. K. Sadananda and P. Shahinian, "Effect of Environment on Crack Growth Behavior in Austenitic Stainless Steels Under Creep and Fatigue Conditions," Metallurgical Trans. A 11A, 267-276 (1980).

29. J. Lanteigne and J. Bailon, "Theoretical Model for FCGR Near the Threshold," Metallurgical Trans. A 12A, 459-466 (1981).

30. J.C. Radon, "A Model for Fatigue Crack Growth in a Threshold Region," Intern. J. of Fatigue, 161-166 (July 1982).

31. J.A. Dalessandro, "Structural Considerations for a Tokamak Fusion Reactor," Nucl. Engr. and Design 39, 141-151 (1976).

32. K. Sadananda and P. Shahinian, "Creep Crack Growth Behavior and Theoretical Modeling," Metal Science 15, 425-432 (1981).

33. K. Sadananda and P. Shahinian, "Review of the Fracture Mechanics Approach to Creep Crack Growth in Structural Alloys," Engr. Fracture Mechanics 15, 327-342 (1981).

34. A. Saxena, "Evaluation of C^* for the Characterization of Creep-Crack-Growth Behavior in 304 Stainless Steel," Fracture Mechanics, Twelfth Conference, ASTM STP 700, American Society for Testing and Materials, (1980), pp. 131-151.

35. G.G. Musicco, "On the Methods to Evaluate J^* for Creep Crack Growth Tests," Intern. J. of Fracture 19, R41-R42 (1982).

36. H. Reidel and J.R. Rice, "Tensile Creeping in Solids," Fracture Mechanics, Twelfth Conference, ASTM STP 700, American Society for Testing and Materials, (1980), pp. 112-130.

37. R.D. Nicholson and C.L. Formby, "The Validity of Various Fracture Mechanics Methods at Creep Temperatures," Intern. J. of Fracture 2, 595-604 (1975).

38. P.L. Jones and A.S. Tetelman, "Characterization of the Elevated Temperature Static Load Crack Extension Behavior of Type 304 Stainless Steel," Engr. Fracture Mechanics 12, 79-97 (1979).

39. S. Taira, R. Ohtani and T. Kitamura, "Application of J-Integral to High Temperature Crack Propagation, Part 1 - Creep Crack Propagation," J. of Engr. Mater. and Tech. 101, 154-161 (1979).

40. K. Krompholz, H. Huthmann, E.D. Grosser, and J.B. Pierick, "Creep Crack Growth Behavior in Air and Sodium for an Unstabilized Austenitic Stainless Steel and Assessment of Evaluation Concepts," Engr. Fracture Mechanics 16, 809-819 (1982).

41. P.T. Heald, G.M. Spink and P.J. Worthington, "Post Yield Fracture Mechanics," Mater. Science and Engr. 10, 129-138 (1972).

42. L.H. Larsson, "Use of EPFM in Design," Advances in Elasto-Plastic Fracture Mechanics, 261-278 (1979).

43. A.R. Dowling and C.H.A. Townley, "The Effect of Defects on Structural Failure: A Two Criteria Approach," Intern. J. of Pressure Vessel and Piping 3, 77-107 (1975).

44. B.A. Bilby, A.H. Cottrell, F.R.S. Swinden and K.H. Swinden, "The Spread of Plastic Yield from a Notch," Proceedings of the Royal Society A 272, 304-314 (1963).

45. D.S. Dugdale, "Yielding of Sheets Containing Slits," J. of Mechanics and Physics of Solids 8, 100-104 (1960).

46. F.M. Burdekin and D.E.W. Stone, "The Crack Opening Displacement Approach to Fracture Mechanics in Yielding Materials," J. of Strain Analysis 1, 145-153 (1966).

47. R.P. Harrison, K. Loosemore, I. Milne and A.R. Dowling, "Assessment of the Integrity of Structures Containing Defects," Central Electricity Generating Board R/H/R6-Rev. 2 (1980).

48. B.J.L. Darlaston, "The Development and Application of the CEGB Two Criteria Approach for the Assessment of the Defects in Structures," Advances in Elasto-Plastic Fracture Mechanics, 319-357 (1979).

49. T.U. Marston, "The EPRI Ductile Fracture Research Program," Advances in Elasto-Plastic Fracture Mechanics, 191-235 (1979).